

Newsletter

No. 176 | Summer 2023

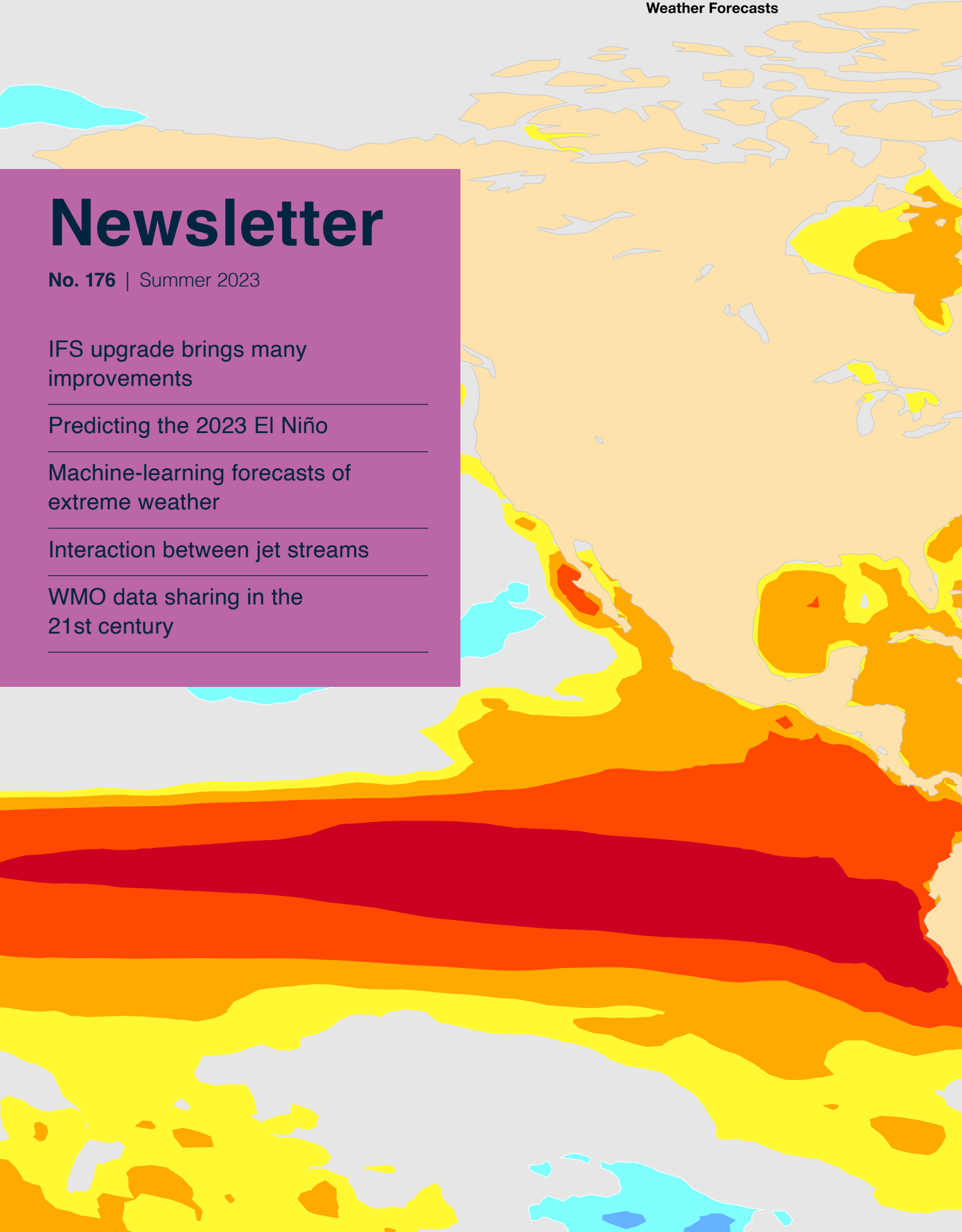
IFS upgrade brings many
improvements

Predicting the 2023 El Niño

Machine-learning forecasts of
extreme weather

Interaction between jet streams

WMO data sharing in the
21st century



© Copyright 2023

European Centre for Medium-Range Weather Forecasts, Shinfield Park, Reading, RG2 9AX, UK

The content of this document, excluding images representing individuals, is available for use under a Creative Commons Attribution 4.0 International Public License. See the terms at <https://creativecommons.org/licenses/by/4.0/>. To request permission to use images representing individuals, please contact pressoffice@ecmwf.int.

The information within this publication is given in good faith and considered to be true, but ECMWF accepts no liability for error or omission or for loss or damage arising from its use.

Publication policy

The ECMWF Newsletter is published quarterly. Its purpose is to make users of ECMWF products, collaborators with ECMWF and the wider meteorological community aware of new developments at ECMWF and the use that can be made of ECMWF products. Most articles are prepared by staff at ECMWF, but articles are also welcome from people working elsewhere, especially those from Member States and Co-operating States.

The ECMWF Newsletter is not peer-reviewed.

Any queries about the content or distribution of the ECMWF Newsletter should be sent to Georg.Lentze@ecmwf.int

Guidance about submitting an article and the option to subscribe to email alerts for new Newsletters are available at www.ecmwf.int/en/about/media-centre/media-resources

Focus on ensembles

An ensemble weather forecast is a set of forecasts that presents the possible range of future weather developments. The main advantage over a single forecast is that it provides information on the uncertainty associated with the forecast, by indicating a range of potential outcomes. The main drawback is that ensemble forecasts are computationally more expensive to produce than single forecasts. For that reason, from 1992 until a few weeks ago we produced high-resolution forecasts (HRES) as well as coarser-resolution ensemble forecasts (ENS) in the medium range. Most recently, the HRES was run at a horizontal resolution of 9 km and the ENS at 18 km. But in a far-reaching upgrade of our Integrated Forecasting System (IFS) to Cycle 48r1 on 27 June, the resolution of our medium-range ENS forecasts was increased to 9 km as well. The upgrade marks an important change in emphasis in favour of ensemble forecasts. As set out in the article on this year's Using ECMWF's Forecasts event, usage of ensemble forecasts still varies among those who took part in the event, but there was broad backing for our emphasis on ensemble-based outputs.

The increase in ENS resolution brought a number of improvements to our forecasts, which are detailed in this Newsletter. But IFS Cycle 48r1 went beyond this change in many ways. It brought many other improvements in data assimilation, to establish the best possible initial conditions for forecasts, and in the forecast model. It also introduced major changes to extended-range ensemble forecasts: their number of ensemble members has increased from 51 to 101, and they are now run daily instead of twice weekly. At the

same time, we upgraded the forecasting system of the EU's Copernicus Atmosphere Monitoring Service (CAMS), which we implement.



The importance of ensemble forecasts can also be seen in the article on the development of El Niño conditions in this Newsletter. Our own seasonal forecasting system, SEAS5, as well as the systems brought together by the Copernicus Climate Change Service (C3S) implemented by ECMWF, uses ensemble forecasts to describe the possible range of future temperature anomalies in the equatorial Pacific Ocean. Another article describes how well our seasonal forecasting system predicted the winter 2022/23 in the face of energy security concerns across the continent in relation to the war in Ukraine. Collaboration in training features prominently, with articles on the OpenIFS User Meeting in Barcelona and support for the ICON training carried out by the German Meteorological Service.

This Newsletter also describes the results of tests carried out at ECMWF of external machine-learning forecasts of extreme weather. They show that machine-learning models can successfully forecast extreme weather situations. These forecasts are currently not available as ensemble forecasts, but this is surely only a matter of time.

Florence Rabier
Director-General

Contents

Editorial

Focus on ensembles 1

News

Predicting the 2023 El Niño event 2
 Predicting tropical cyclone Mocha in the Bay of Bengal 4
 Post-processing ERA5 output with ecPoint 6
 Exploring machine-learning forecasts of extreme weather . . . 8
 Biggest ever UEF focuses on ensemble forecasting 10
 User support surveys for Copernicus and commercial users 12
 OpenIFS user meeting focuses on atmospheric composition 13
 How well did we forecast the winter 2022/23? 14
 ECMWF supports DWD ICON training 16
 Major upgrade of CAMS forecasts of atmospheric composition. 17

Increased use of surface observations 18
 Open data community mailing list 20
 New observations April – June 2023 20

Earth system science

IFS upgrade brings many improvements and unifies medium-range resolutions 21
 Interaction between polar and subtropical jet streams over Greece, 7–10 July 2022 29

Computing

WIS 2.0: WMO data sharing in the 21st century 35

General

ECMWF publications 40
 ECMWF Calendar 2023/24 40
 Contact information 40

Predicting the 2023 El Niño event

Tim Stockdale

ECMWF forecasts and forecasts provided by the EU-funded Copernicus Climate Change Service (C3S) implemented by ECMWF have been consistent throughout the first half of 2023 in indicating the development of an El Niño event, which is now in progress. The first figure shows how the El Niño might look later this year, and the second figure shows successive ECMWF forecasts for the NINO3.4 region. Despite the accuracy of these forecasts so far, we know that forecasting El Niño is sometimes tricky. What are the uncertainties in our forecast, and how can we assess them?

Main uncertainties

The most basic uncertainty on seasonal timescales stems from unpredictable wind variations over the equatorial Pacific, which can be quite large scale in both space and time (10s of days and 1,000s of kilometres). The zonal component of these wind variations along the equator strongly affects the ocean dynamics, driving substantial variations in NINO index sea-surface temperatures (SSTs). We account for this uncertainty by running ensemble forecasts – the details in each ensemble member evolve differently, and we obtain a ‘plume’ of forecast

What is El Niño?

El Niño is a large-scale heating of the equatorial Pacific Ocean. Under normal conditions, a cold tongue of upwelled water extends along the equator from Peru and Ecuador towards the date line. The upwelling is driven by easterly trade winds along the equator, which in turn are driven by

large amounts of deep convection over the western Pacific and Indonesia. In El Niño conditions, the cold tongue warms up, deep convection moves eastwards towards the central Pacific, and the trade winds weaken. These processes reinforce each other, producing a sustained change in the atmospheric circulation with impacts across the globe.

SST values. The ensemble is constructed to take account of uncertainties in the initial conditions for both atmosphere and ocean, but it is in fact the wind variability during the forecast that dominates the spread between ensemble members.

Taken at face value, the plume from our latest July forecast suggests we can expect a moderate El Niño event peaking at 1.5°C, or a very large event of 3°C, or anything in between (see the second figure). But is it this simple?

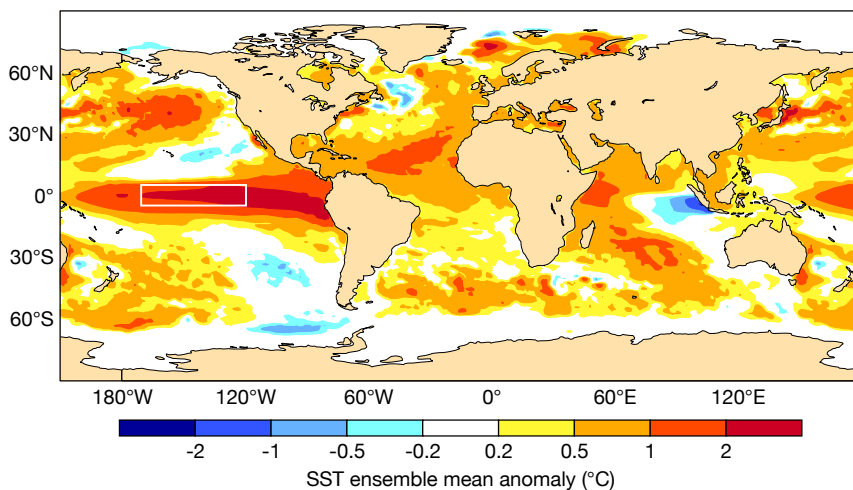
Forecast models are imperfect, and although remarkably realistic in many aspects even when integrated for a year or more, they develop various biases and subtle distortions. For El Niño, even small differences in temperature gradients can have a substantial impact on atmospheric

evolution, and model imperfections inevitably lead to errors in the forecast plume. Our representation of initial condition uncertainty, particularly in the ocean, is also imperfect. It is thus no surprise that when we compare the ensemble spread, averaged over many cases, with the average root-mean-square forecast error, we discover that for SST indices such as NINO3.4, the error is bigger than the spread. Our real-time forecast uncertainty is thus (on average) larger than the spread of the forecast plume, and detailed information on this is provided by verification plots on our website.

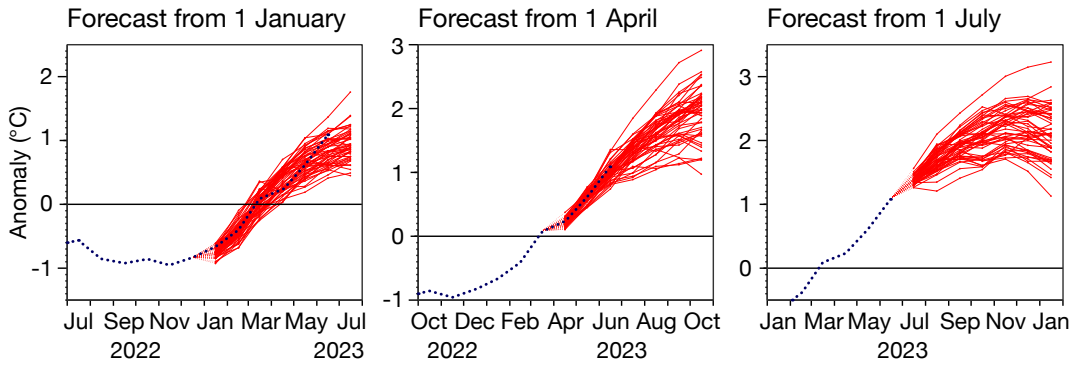
The width of the plume could be inflated to match the overall level of forecast error seen in past cases, but there is ambiguity in how this might best be done. Physically, the impact of model imperfections is not random but state-dependent, so how a specific forecast such as that of 2023 might be affected is unclear. There are not enough past cases to create a state-dependent probabilistic calibration of our forecast models, so how to proceed?

Value of multi-system forecasts

A valuable method is to combine the results from multiple forecast systems, which is the aim of the C3S multi-system seasonal forecast (see the third figure). Forecast errors introduced by model imperfections differ across models, so by averaging results the error in the ensemble mean forecast is reduced. The use of different ocean analyses also improves the representation of ocean initial



SST ensemble mean anomaly forecast. The chart shows the SST ensemble mean anomaly forecast from July 2023 for October–November–December 2023, according to ECMWF’s seasonal forecasting system SEAS5. The NINO3.4 region is indicated by the box.



ECMWF forecasts. Here we show NINO3.4 SST anomaly plumes from 1 January, 1 April and 1 July 2023, according to ECMWF's SEAS5 system. The blue dots show the observed SST anomaly, and the red lines show the forecast for the next seven months.

condition uncertainty. Further, the spread between different forecast systems can give guidance on the robustness of any signals present. Using multiple forecast systems is a rather ad hoc method of sampling uncertainties and does not automatically result in a well-calibrated probability distribution function. However, experience shows it gives robust improvement in both skill and statistical reliability of seasonal forecasts.

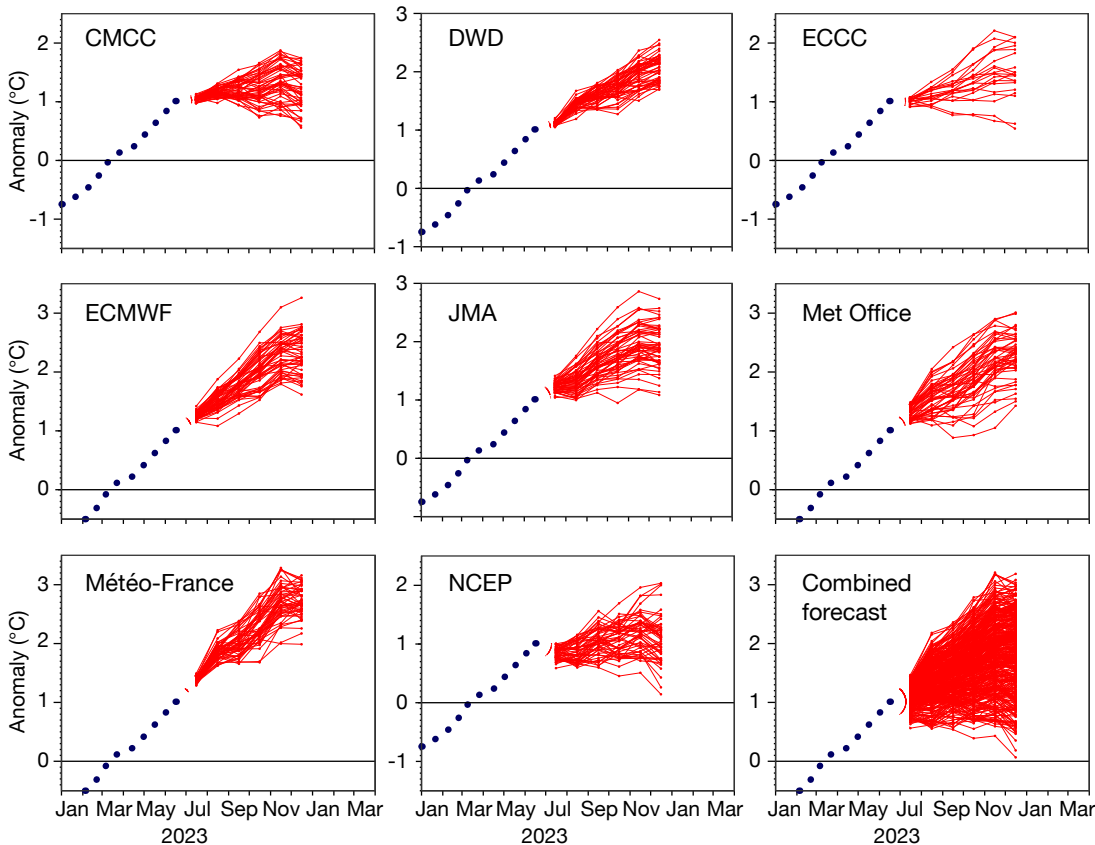
Influence of a changing climate

A final source of uncertainty is the rapidly changing Earth system climate. Our calibration and error estimations come from the past, and although ECMWF's seasonal

forecasting system SEAS5 and other models capture global warming trends well, some recent regional trends in the tropics appear to be wrong. Examples include small trends in upper-air wind shear over the Atlantic and SST in the eastern equatorial Pacific, which in recent years has tended to be cooler than model predictions, due to stronger than expected winds. Some of this might be chance, but there might be systematic problems in our models, such as inadequate cloud feedbacks, failure to represent tropical deforestation and biases interacting with changes in observing systems. Different calibration choices would affect the amplitude of the predicted 2023 El Niño – it would be

0.2 degrees less if we used only the last ten years of data, for example, rather than the 1993–2016 period. A final source of uncertainty is stratospheric water vapour injected by the unprecedented Hunga Tonga eruption in 2022 – this is expected to give additional modest warming on a global scale, but any possible impact on El Niño is unknown.

Despite all these unaccounted-for uncertainties, the biggest factor determining the size of the El Niño is still likely to be unpredictable variations in the wind, for which our plumes give reasonable guidance. The future will tell whether the El Niño of 2023 exploded, developed more moderately, fizzled, or even became a slow-burn two-year event.



C3S forecasts. These are the NINO3.4 SST anomaly plumes from 1 July 2023 according to the C3S website. The bottom-right panel shows the combined forecast. The forecasts are from Italy's Euro-Mediterranean Center on Climate Change (CMCC), the German Meteorological Service (DWD), Environment and Climate Change Canada (ECCC), ECMWF, the Japan Meteorological Agency (JMA), the UK Met Office, Météo-France and the US National Centers for Environmental Prediction (NCEP). (Credit: Copernicus Climate Change Service/ECMWF)

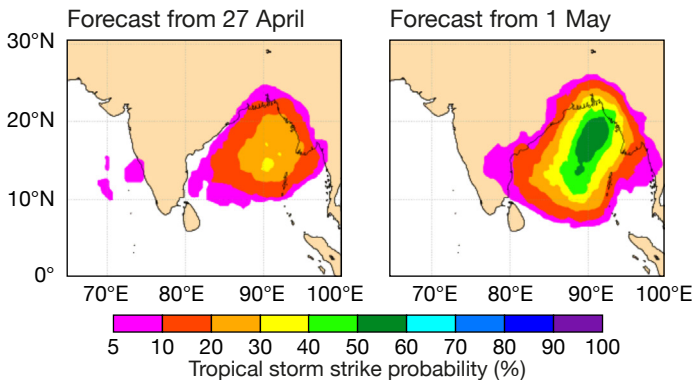
Predicting tropical cyclone Mocha in the Bay of Bengal

Linus Magnusson, Mohamed Dahoui, Cristina Prates

On 14 May 2023, tropical cyclone (TC) Mocha made landfall in Myanmar and impacted Bangladesh. During part of the track, the cyclone was one of the strongest ever in the Bay of Bengal. Significant evacuations were made ahead of the cyclone.

Forecasts of TC Mocha

The cyclone formed on 11 May in the southern Bay of Bengal. The area had a lot of convection in the week before, probably connected to the passage of a Madden–Julian Oscillation at the end of April and an active equatorial Rossby wave in the region. The extended-range forecast from as early as 27 April predicted increased probability of tropical cyclone activity in the Bay of Bengal for 8–15 May (see the first figure). The probability increased in the forecast from 1 May and was consistently above 50% in subsequent forecasts. This makes



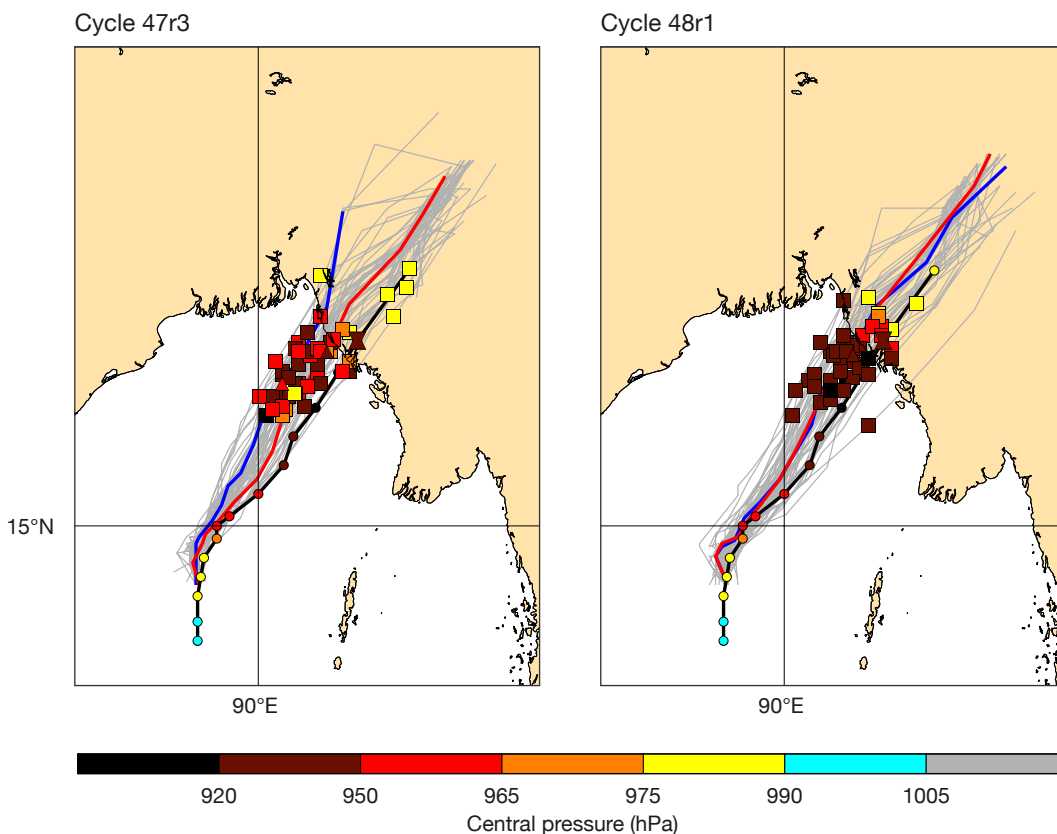
Extended-range forecasts.

Tropical storm strike probabilities for 8–15 May in extended-range forecasts from 27 April (left) and 1 May (right).

the genesis of TC Mocha one of the most predictable in recent years.

After the formation of the cyclone, there were still large uncertainties both in terms of the landfall position on the eastern side of the Bay of Bengal and the intensity. The ECMWF ensemble predicted the landfall to be too far north along the coast one to three days before landfall, as can be seen in the example from 12 May

00 UTC. The forecasts also predicted a later landfall than observed, which is a result of a known slow-propagation-speed bias in ECMWF forecasts. With the upgrade of the ECMWF ensemble to 9 km resolution (Cycle 48r1), there is now an increased capability to predict tropical cyclone intensity and to give a better estimate of the uncertainties. As can be seen in the second figure,



TC Mocha in Cycle 47r3 and Cycle 48r1.

Forecast for TC Mocha from 12 May 00 UTC in operational forecasts using Cycle 47r3 (left) and pre-operational forecasts using Cycle 48r1 (right). The black line represents BestTrack observations (with coloured dots every 6th hour), the red line the high-resolution forecast (HRES), the blue line the control of the ensemble forecast (ENS), and the grey lines the ENS members. Position and intensity on 14 May 12 UTC are shown by the hourglass symbol for BestTrack, triangles for HRES and ENS control and squares for the ensemble members.

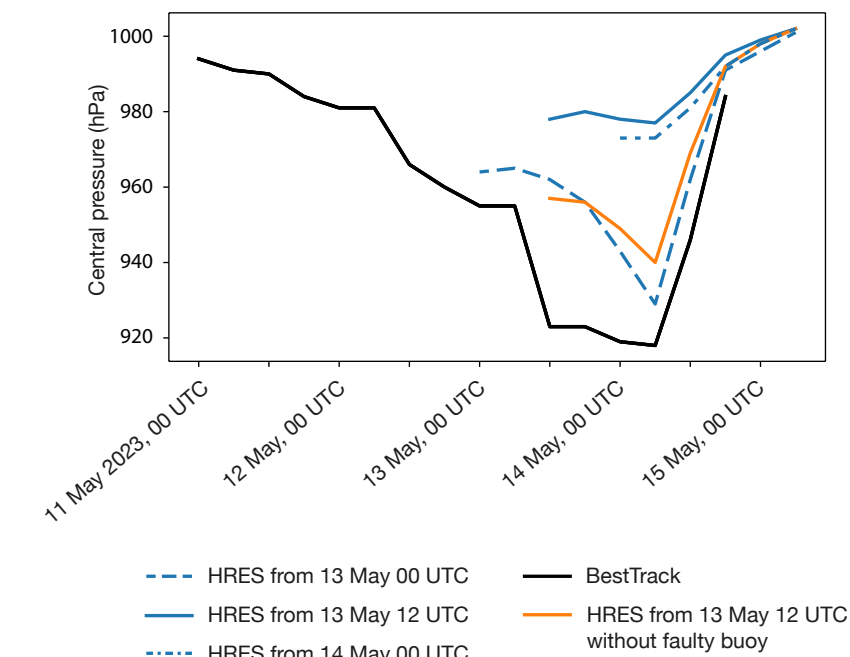
such an improvement is reflected in the medium-range prediction of intensity in the Cycle 48r1 ensemble. It can also be seen that the trajectory prediction is slightly better in Cycle 48r1 than in Cycle 47r3, which was operational at the time.

Faulty buoy

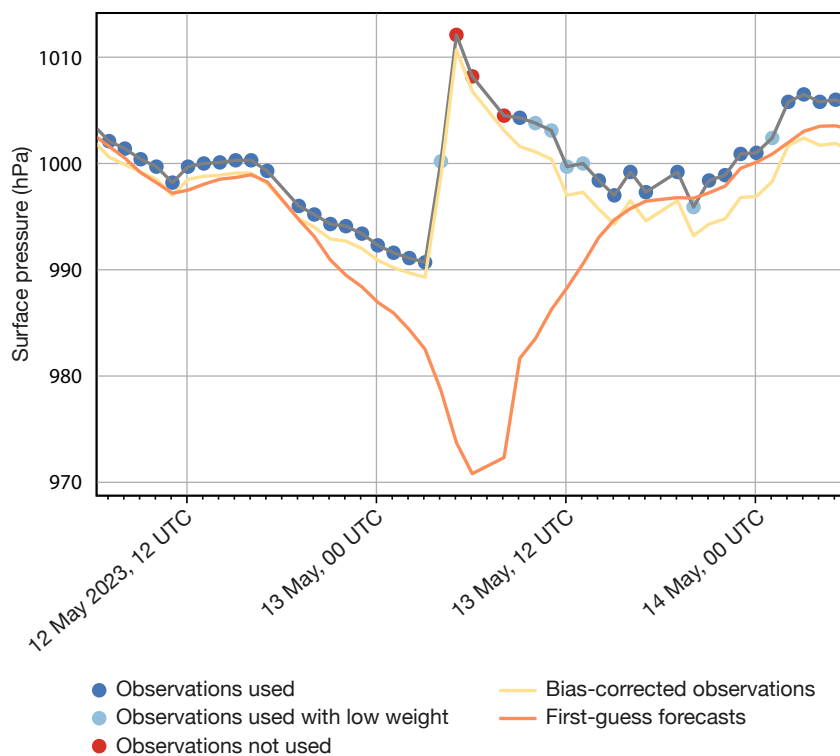
In the forecasts (both operational and pre-operational) from 13 May 12 UTC, i.e. one day before landfall, the cyclone became much weaker, while in reality it continued to increase its strength (see the third figure). The erroneous intensity affected subsequent high-resolution forecasts (HRES) as well as ensemble forecasts (ENS). Investigations afterwards at ECMWF found one meteorological buoy in the path of the cyclone that suddenly reported increasing pressure during the passage instead of decreasing pressure. The buoy was sending observations every hour, meaning that several observations entered the data assimilation. The buoy had been problem-free before the cyclone. Even though observations from the buoy were picked up by the quality control in the data assimilation as problematic, they were used to some degree during the period concerned (see the fourth figure). An experiment afterwards without the buoy confirmed that it was the source of the degraded intensity forecast. Instrument faults during the harsh conditions under a tropical cyclone are very difficult to detect in data assimilation, particularly because we expect large uncertainties in the forecasts, and we want to use as much (good) information as possible from the few available surface observations. But work continues to improve resistance to this type of error.

Conclusion

The case of tropical cyclone Mocha illustrates forecast challenges on different timescales. While the cyclone was relatively predictable regarding the genesis, the medium- and short-range forecasts had difficulties both with track and intensity predictions. This was made worse by the assimilation of the surface pressure from a faulty buoy. Nevertheless, as a result of forecasts



Central pressure forecasts and BestTrack. The chart shows central pressure for TC Mocha in BestTrack and operational HRES forecasts from 13 May 00 UTC, 13 May 12 UTC, and 14 May 00 UTC. The forecast from analysis without faulty buoy from 13 May 12 UTC is also shown.



The buoy in the Bay of Bengal. The chart shows a time series of bias-corrected observations from the buoy in the Bay of Bengal, first-guess forecasts, and the usage of observations in the data assimilation system.

from ECMWF and other centres, significant evacuations took place

before landfall and likely prevented loss of human life.

Post-processing ERA5 output with ecPoint

Tim Hewson, Fatima Pillosu, Estíbaliz Gascón, Milana Vučković

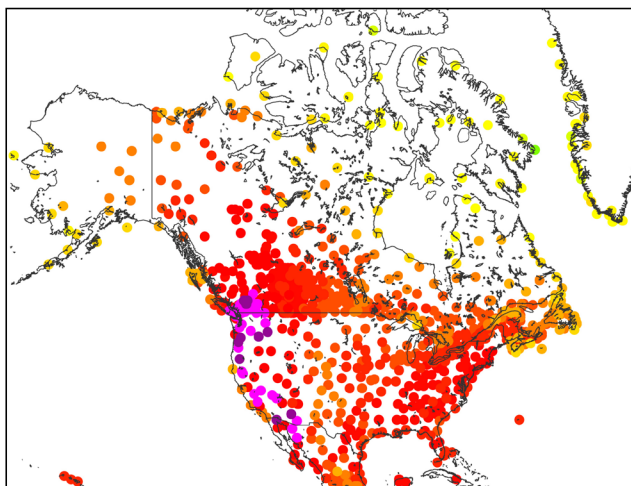
Observation-based climatologies help detect trends and patterns in the climate over a long period of time and can contextualise extreme, high-impact weather events. However, observations can be inaccurate and are unevenly distributed in space and time. The ERA5 reanalysis, which is produced by the Copernicus Climate Change Service (C3S) run by ECMWF and is based on state-of-the-art data assimilation and numerical weather

prediction (NWP), provides an alternative: an accurate, temporally consistent, gridded estimate of the past state of the Earth system worldwide. However, this does not satisfy all needs due to ERA5's relatively coarse model resolution, which precludes representation of localised extremes, and because of some intrinsic biases.

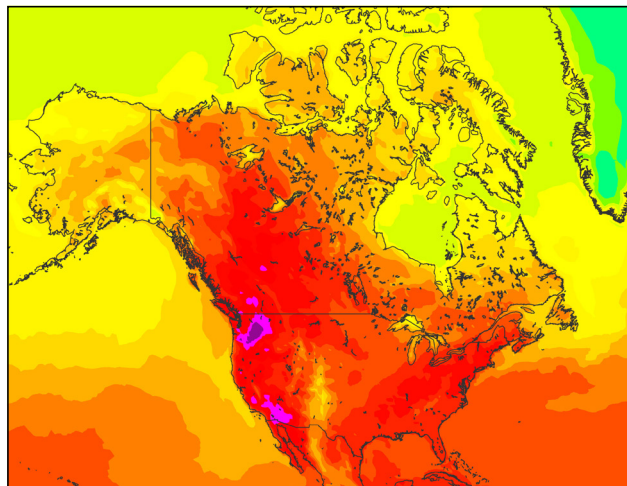
Within the Highlander project, co-financed by the EU and

coordinated by Italy's Cineca computing centre, ECMWF's ecPoint post-processing technique was applied to raw ERA5 'deterministic' fields to address ERA5 limitations. ecPoint is formulated for independent application to any single model realisation and aims, in particular, to infer sub-grid variability and to correct biases (both according to ongoing weather and geographical scenarios). So in this way we create

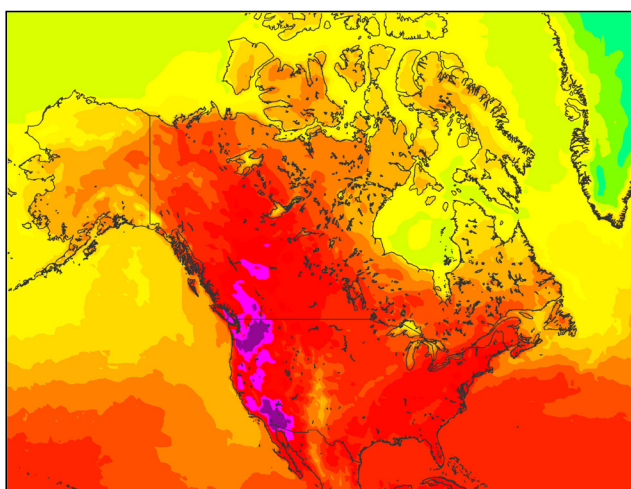
Observations



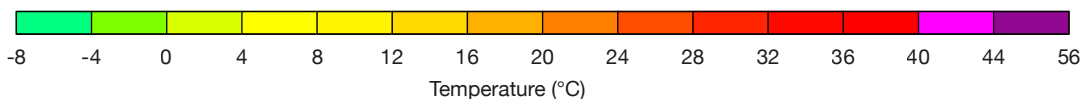
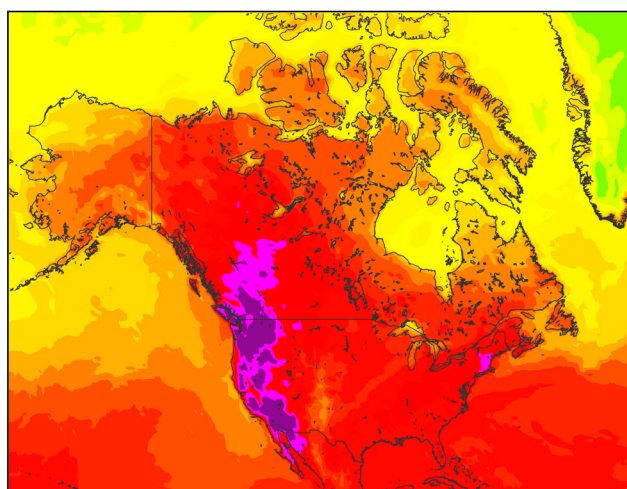
ERA5



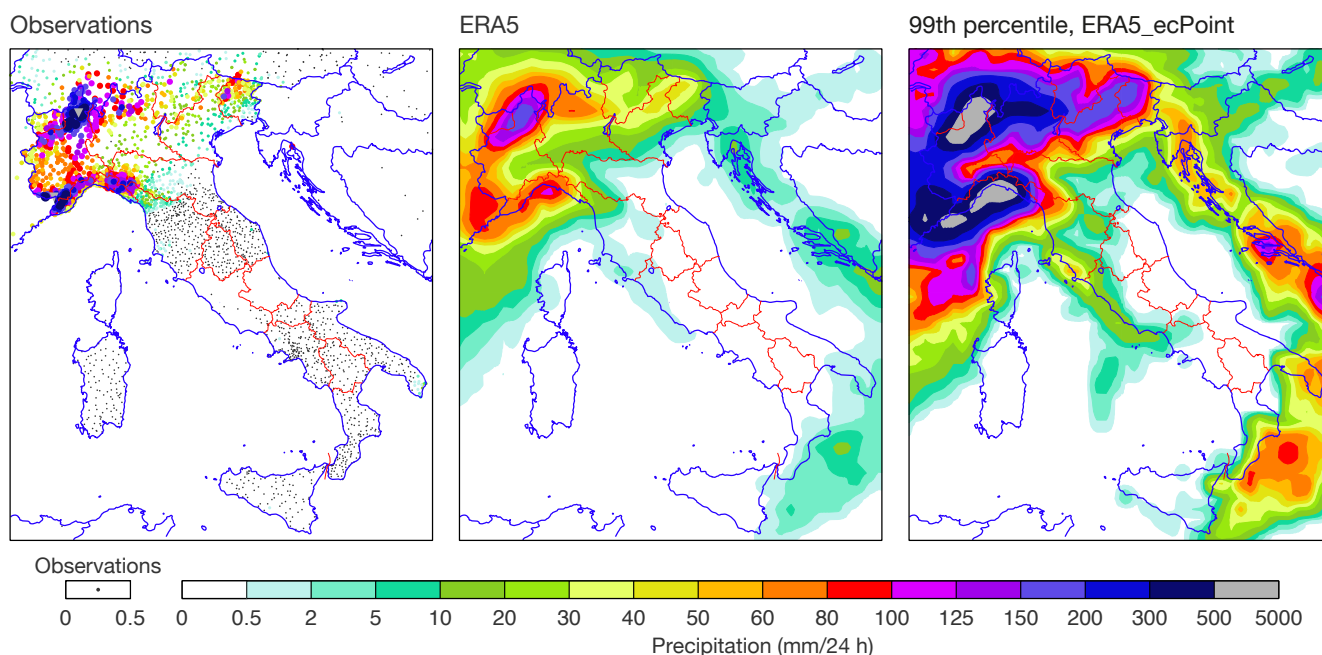
Bias-corrected, ERA5_ecPoint



90th percentile, ERA5_ecPoint



Maximum 2-metre temperature in 24 hours ending at 00 UTC on 29 June 2021. The top panels show SYNOP weather station observations (left) and the ERA5 reanalysis (right). The bottom panels show bias-corrected ERA5_ecPoint (grid scale, left) and the 90th percentile of ERA5_ecPoint (for point scale, right).



Precipitation in 24 hours ending at 00 UTC on 3 October 2020. The panels show SYNOP weather station observations (left), the raw ERA5 reanalysis (centre), and the 99th percentile of ERA5_ecPoint (right).

much more reliable (probabilistic) point-scale climatologies.

ERA5_ecPoint has so far been created for 1950 to 2021, for 24- and 12-hourly rainfall, and 24 h minimum, maximum, and mean 2 m temperature. Two product classes were developed: grid-scale bias-corrected ('deterministic') and point-scale (probabilistic; percentiles 1 to 99). Currently provided on its native (reduced Gaussian) grid, with a spatial resolution of approximately 31 km (TL639), ERA5_ecPoint data should be added to the Copernicus Climate Data Store later this year. At present only an Italian cut-out region is accessible, through the Highlander data portal.

Example 1: Maximum 2-metre temperatures during a heatwave over western North America in June 2021

Between late June and early July 2021, an extreme heatwave brought temperatures over 40°C to western parts of both Canada and the USA, causing billions of dollars in damage to agriculture, infrastructure, and the environment, and impacting people's health. The most notable maximum temperature record was 49.6°C in Lytton, Canada, on 28 June.

Although raw ERA5 signalled extreme heat in western North America, it could not identify the full spatial extent or the

extreme temperatures associated with the event. This is believed to be due mainly to unresolved local topographic details. So, whilst raw ERA5 captured well extreme temperatures in flatter areas such as the Columbia plateau in the north-western USA, in more mountainous regions it markedly underestimated them (e.g. giving 37°C for Lytton). Due to corrections specifically targeting areas with complex orography, the extent of very high temperatures in the bias-corrected ERA5_ecPoint matches observations more closely than does the raw ERA5. However, for an even better observation match one needs the probabilistic point-scale output. For example, the 90th percentile, which should be exceeded by 10% of observations, captured local extremes rather better (e.g. giving 48°C in Lytton). The first figure shows the results of applying ecPoint to ERA5 for 28 June.

Example 2: Extreme rainfall over Italy, 2 October 2020

In early October 2020, Storm Alex brought strong winds, heavy rain and thunderstorms to south-eastern France, northern Italy, and Central Europe, causing landslides and widespread severe flooding. Houses and infrastructure were very badly affected and there were 15 fatalities.

As in the temperature example, ERA5

rainfall output signalled extreme conditions, over north-western Italy for example, but did not capture local extrema. The highest values measured (around 600 mm/24 h) can be attributed to interactions between organised convection and the Alps. Raw ERA5 estimates for 2 October did not exceed 200 mm/24 h, likely due to convective parametrization limitations, sub-grid variability and biases related to topographic complexity. Meanwhile the ERA5_ecPoint 99th percentile peaked around 600 mm/24 h, because it targets factors such as these. The second figure shows the 99th percentile of ERA5_ecPoint for 2 October.

Summary and usage

ERA5_ecPoint nicely complements ERA5 for surface weather parameters, by correcting for biases and by providing probabilistic metrics. Whilst value should be added worldwide, users can benefit most where observations are lacking. ERA5_ecPoint also catalogues situation-dependent ERA5 grid-scale biases, and additionally it provides point-scale metrics to compare forecasts with, e.g. for rainfall warnings. Users will doubtless find other applications. Whilst further direct verification of ERA5_ecPoint is desirable, initial work indicates that the wet tails of station-based rainfall climatologies are well represented.

Exploring machine-learning forecasts of extreme weather

Linus Magnusson

Over the last few years, developments in data-driven numerical weather prediction (NWP) based on machine learning have been very fast. A common setup is to use ECMWF’s ERA5 reanalysis to train global models for medium-range forecasting. These work in a similar way to a conventional model, in the sense that they are initialised from an analysis and step forward in time using a model.

Two of these models have been made public, namely Huawei’s Pangu-Weather (PGW hereafter) and NVIDIA’s FourCastNet. In the last few months, ECMWF staff have built infrastructure to run these models. They can now be run from our archived data as initial conditions, with the output saved in standardised formats and connected to our verification tools.

For evaluation purposes, ECMWF has run 10-day forecasts initialised from our operational analysis, with output every six hours. For upper-air verification scores, such as 500 hPa geopotential height, PGW shows very competitive results compared to high-resolution forecasts (9 km horizontal resolution – HRES) of ECMWF’s Integrated Forecasting System (IFS) in Cycle 47r3, in other words before the recent upgrade to

Cycle 48r1. In this article, we will revisit two extreme cases from the past year to examine the ability of the PGW data-driven model to produce forecast extremes.

Storm Eunice in February 2022

Storm Eunice hit north-western Europe on 18 February 2022 and was covered in ECMWF Newsletter No. 171. The cyclone formed on 16 February from a baroclinic wave west of the Azores. It quickly intensified on 17 February before reaching southern Ireland around 18 February 00 UTC. Later that day, the cyclone caused extreme winds over the southern UK.

The PGW model captured the development of the cyclone well, e.g. in the forecast from 16 February 00 UTC, initialised before the cyclogenesis of Eunice. In that forecast, the minimum pressure at 00 UTC on 18 Feb reached 969 hPa in PGW, compared to 978 hPa in IFS-HRES, 974 hPa in the ECMWF analysis and 976 hPa in the ERA5 reanalysis. The progress of the cyclone was somewhat faster in PGW than in IFS-HRES and in reality, and the cyclone reached its most intense

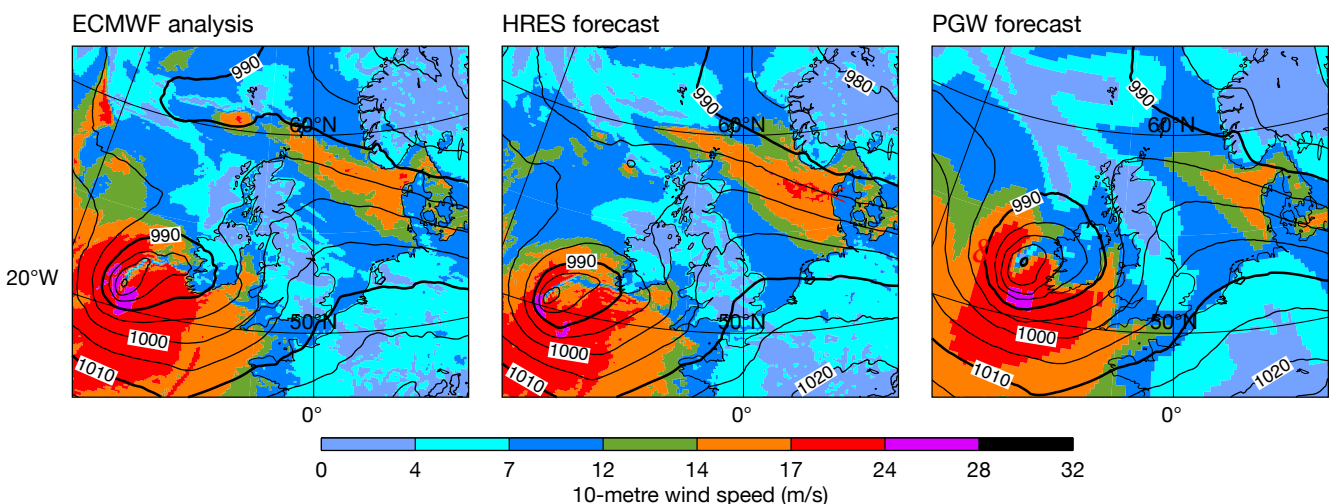
stage earlier. Also, in the first image one can see that PGW is missing some of the small-scale structures that are present in IFS-HRES (and in the analysis), such as increased winds along the trough south of the cyclone.

For medium-range forecasts, PGW gave a clear indication of extreme wind 4–5 days in advance, on a similar range as ECMWF forecasts (not shown). However, the maximum wind was somewhat underestimated in PGW for the southern UK and over the English Channel.

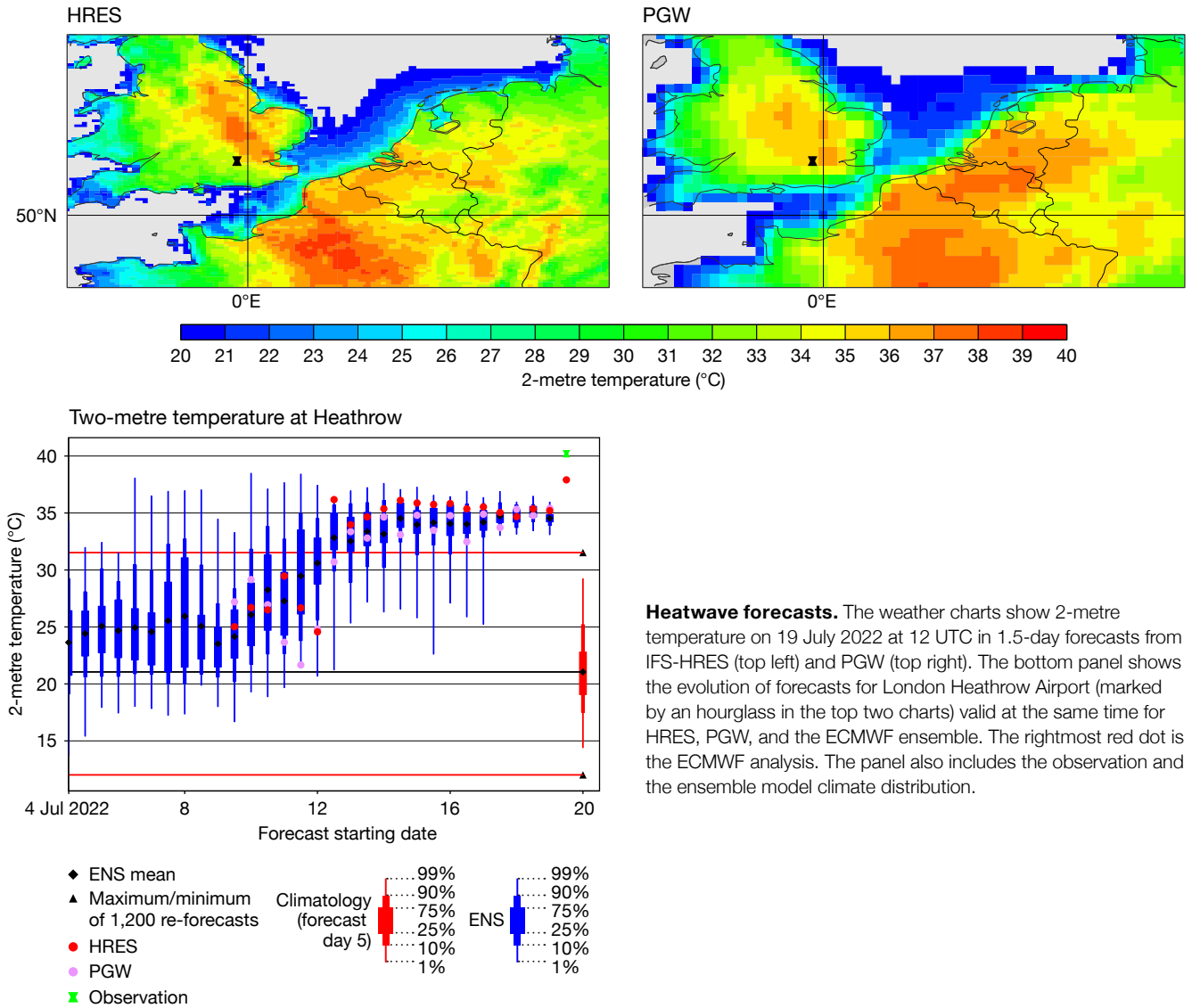
This example shows that PGW is capable of producing very intense extra-tropical cyclones, but it can underestimate maximum wind speeds. The latter is possibly the result of a lack of fine-scale structures in the forecasts, due to the training methodology used to create the model.

UK heatwave in July 2022

In the summer of 2022, the UK reached 40°C for the first time on 19 July (see ECMWF Newsletter No. 173). At 12 UTC on that day, the warmest station was London Heathrow Airport with 40.2°C (later 40.3°C was reached in Coningsby, Lincolnshire). Evaluating the 12 UTC temperature for London Heathrow



Pressure and wind speed for Storm Eunice. Mean sea-level pressure (contours, in hPa) and 10-metre wind speed (shading) for Storm Eunice valid on 18 Feb 2022 at 00 UTC in ECMWF’s analysis (left) and in 48-hour forecasts from IFS-HRES (middle) and PGW (right).



Heatwave forecasts. The weather charts show 2-metre temperature on 19 July 2022 at 12 UTC in 1.5-day forecasts from IFS-HRES (top left) and PGW (top right). The bottom panel shows the evolution of forecasts for London Heathrow Airport (marked by an hourglass in the top two charts) valid at the same time for HRES, PGW, and the ECMWF ensemble. The rightmost red dot is the ECMWF analysis. The panel also includes the observation and the ensemble model climate distribution.

Airport from earlier forecasts, we see that the ensemble forecast (ENS) predicted warmer than normal temperatures more than 15 days before. Around 10 days before the event, ENS became warmer, and from seven days before the event (12 July 12 UTC) and onwards, the ENS mean was above the maximum from the 20-year model climate for this time of the year. However, compared to the observed 40.2°C, even the shortest-range forecasts before the event fell short, being around 35°C.

For PGW, although it is a deterministic forecast, the evolution of the predictions followed the trend of the ensemble distribution. From 13 July 00 UTC and onwards, the PGW prediction was above the maximum of the ECMWF model climatology, and for shorter forecasts it was well centred in the ensemble. However,

one can note a flip-flopping pattern for PGW, with forecasts initialised at 00 UTC being slightly warmer than those initialised at 12 UTC.

Comparing spatial patterns of 2-metre temperature in the 1.5-day forecast, one can see that PGW appears to be smoother than ECMWF HRES, and also to predict lower maxima over both the UK and France, which both had a very extreme heatwave. The smoothing is partly due to lower resolution (about 27 km in the model and the training dataset, compared to 9 km for HRES) but could also be due to the way the model is trained.

Summary

Using cases in ECMWF's Severe Event Catalogue, we have started to evaluate machine-learning forecasts of extreme cases, alongside statistical evaluation. In this short article, we have looked back at two such cases

from 2022 over Europe. The two examples used here show that data-driven models are capable of forecasting extreme weather situations and of providing guidance in the medium range.

The PGW model does not produce forecasts for precipitation, clouds, visibility, wind gusts, etc., which has limited our investigations. Also, there is no reliable ensemble method available yet, due to missing model uncertainty, which is why we have not evaluated that aspect. Future developments of data-driven models are likely to target these shortcomings.

For more details, see the ECMWF science blog on the rise of machine learning in weather forecasting: <https://www.ecmwf.int/en/about/media-centre/science-blog/2023/rise-machine-learning-weather-forecasting>.

Biggest ever UEF focuses on ensemble forecasting

Becky Hemingway

This year's Using ECMWF's Forecasts (UEF2023) event was held at ECMWF's headquarters in Reading, UK, between 5 and 8 June. The event was in-person with a livestream. This allowed a record number of people to attend: around 80 came to Reading and up to 80 attended online at any one time. The event had a welcoming atmosphere and interesting discussions were had throughout. UEF events aim to provide a forum for exchanging ideas and experiences on the use of ECMWF data and products, and this was successfully achieved.

This year's theme was 'Ensemble Forecasting' and focused on four thematic areas: the science of ensemble forecasting, using ensemble models and data, ensemble forecast applications and products, and communication of ensembles and probabilities. The theme was well placed as ECMWF recently celebrated 30 years of ensemble forecasting. The importance of the theme to users was clear, with many presentations talking about how ensembles are used for a large variety of topics covering meteorology, hydrology and climatology.

Meeting highlights

With Cycle 48r1 of ECMWF's Integrated Forecasting System (IFS) being close to implementation at the time, many of the updates from ECMWF highlighted the changes and improvements brought by this new

cycle. Florian Pappenberger, Director of Forecasts at ECMWF, gave an overview of the changes and showed a positive scorecard for multiple model fields. Matthieu Chevallier, Head of Evaluation at ECMWF, provided an overview of new and updated ECMWF products available in Cycle 48r1. Speaker's Corner went into more detail, with presentations covering: meteograms, including a new visibility meteogram (Cihan Sahin, ECMWF); convective products (Ivan Tsonevsky, ECMWF); the new freezing drizzle precipitation type (Tim Hewson, ECMWF); extended-range forecasts (Fernando Prates, ECMWF); and a new snow scheme (Gabriele Arduini, ECMWF).

Stephen English, Deputy Director of Research at ECMWF, went further into the future and presented research plans for Cycle 49r1 and beyond, including 2 m temperature improvements, the possibility of hourly data assimilation updates, and major changes to the ensemble system (ENS).

Throughout the event, many areas of ensemble forecasting were presented. Chiara Marsigli (German Meteorological Service and Italy's Arpae-SIMC) showed how ensemble resolution changes what is forecast, and how to indicate the possible occurrence of severe weather, even with low probability. Ken Mylne (Met Office, UK) gave an overview of how ensembles are exploited at the Met Office and of future plans, including

supporting users with their use and communication of ensemble data. Simon Boardman (Met Office, UK) showed how ECMWF data are integrated into the Met Office system from a technical perspective and the challenges faced with this.

Communication of ensemble information to users and decision-makers is crucial. Patrick Campbell (University of Oklahoma, USA) presented the Probabilistic Hazard Information (PHI) tool and how it is used to improve the communication of tornado, hail and lightning warnings in the USA. Matteo Ponzano (Météo-France) discussed how understanding end user cost/loss ratios can improve both the products issued and user decision-making. Kosuke Ono (Japan Meteorological Agency) and Robert Neal (Met Office, UK) both presented clustering techniques as a way to summarise ensemble data for easier communication.

Alexandre Trajan (Météo-France) gave a forecaster perspective on the use of ensemble models and how they are used to provide weather warnings in France. Pdraig Flattery (Met Éireann – the Irish Meteorological Service) presented a poster on the use of ensemble data in case studies of storms and heavy precipitation events in Ireland.

The prominence of machine learning has considerably increased over the last few years throughout the meteorological community. Florian



In-person attendees. UEF2023 welcomed in-person attendees as well as online participants.

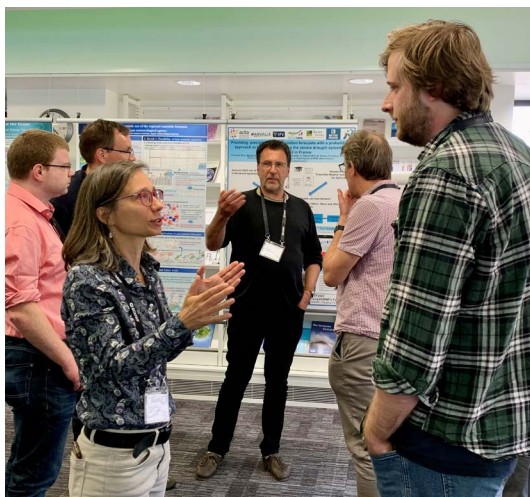
Pappenberger provided an overview of what the ECMWF Machine Learning Roadmap has achieved so far and acknowledged machine learning's busy and fast-evolving landscape. This means ECMWF's Strategy will be revised as ECMWF needs to adapt to progress in the area.

In the Ensemble and Machine Learning session, Mariana Clare (ECMWF) presented a methodology for producing reliable and skilful post-processed probabilistic forecasts without requiring ensemble information. Forest Cannon (Tomorrow.io) showed how a multi-task neural network forecast can outperform the US National Oceanic and Atmospheric Administration High-Resolution Rapid Refresh (HRRR) model. Federico Grazzini (Ludwig Maximilian University of Munich, Germany/Arpa-SIMC, Italy) presented the MaLCox model and demonstrated how it can support extreme precipitation forecasting in Italy. Linus Magnusson (ECMWF) compared the Pangu-Weather and FourCastNet machine learning models with ECMWF's IFS. Harilaos Loukos (The Climate Data Factory, France) presented how machine learning can help to predict sub-seasonal drought and heatwaves.

An ensemble of discussions

On Wednesday afternoon, a new UEF approach was tried: 12 questions exploring forecasting, research, data, and outreach with a focus on ensembles were spread across various rooms. For each of the questions, attendees were invited to 'vote' with dot stickers, comment using post-its, or discuss with ECMWF experts (or a combination of the three). The aim was to generate discussion, gauge user preferences for future work, and gather general feedback. The session exceeded expectations: discussions and debate were plentiful, the sticker 'voting' worked very well, and a plethora of feedback was gathered.

Additionally, throughout the event, a similar approach was used to ask attendees more general questions on the ECMWF website, training, products, and the UEF, with the aim to gather feedback in these areas. Again, this provided useful ideas and feedback for future activities.



In the Weather Room.

Attendees debate an issue during 'Group discussions on the use of ensembles'.

User Voice Corner

The annual User Voice Corner sent a survey to registered UEF2023 participants. The survey gathers feedback on ECMWF forecasts and forecast products. Survey responses are summarised and presented during UEF. It was clear that respondents continue to value and use medium-range ensemble forecasts, particularly for precipitation, wind and temperature, with many happy with quality and forecast skill. Some forecast issues were raised: Croatia highlighted some erroneous turbulence forecasts; Indonesia showed 'stripy' seasonal forecast (SEAS5) rainfall outputs; and errors in temperature were shown across the Alps, which were suspected to be due to station vs model height differences. In line with the UEF2023 theme, respondents were asked about their usage of deterministic vs ensemble data. Answers were varied: some use deterministic more, some use more ensembles, and some use deterministic at short lead times and ensembles at longer lead times. Most supported the ECMWF strategy of more ensemble-based outputs, but it was noted that this needs to be backed up with supporting activities.

Re-forecasting session

A lot of work has been done at ECMWF regarding re-forecasting, especially given the increased resolution of medium-range ensembles and greater ensemble size of extended-range ensembles in Cycle 48r1. Magdalena Balmaseda (ECMWF) provided an overview of current configurations and options for new configurations coming in Cycle 49r1. It was shown that lagged extended-range forecasts give better

skill in weeks 3 and 4, but not in week 1. The proposed configuration for SEAS6 was also shown. It provides a more comprehensive set of re-forecasts as it is run more frequently, with more members and for longer than the current SEAS5 configuration. Reduced noise and improved forecast accuracy was shown, including skill to 18 months and better El Niño–Southern Oscillation (ENSO) predictability. Dominik Büeler (ETH Zurich, Switzerland) gave a user perspective showing re-forecast skill for 2 m temperature and ongoing work on defining climatological re-forecast distributions to identify extreme temperatures in individual ensemble members. The presentations were followed by a plenary session which discussed biases, flow-dependent calibration and balancing resources between real-time forecasts and re-forecasts.

A 'very useful' event

Feedback during and after the event has suggested that UEF events are valuable for users to learn about the latest updates and developments in ECMWF products and services, and about future projects and areas of attention. Attendees highly valued the in-person, interactive, and networking aspects of UEF2023 as they provided opportunities for engagement across the community, strengthening cross-organisational links, and improving user understanding. The theme was described as relevant and useful, with some asking for a similar theme in the future. Feedback received included: "Thank you for organising this event, I really enjoyed it and found it very useful!" and "Thank you so much for this very inspiring meeting."

User support surveys for Copernicus and commercial users

Ruth Coughlan, Anabelle Guillory, Xiaobo Yang

In recent years, ECMWF has introduced some significant changes to the support services it provides to its users. To better understand the impact this has on ECMWF users and how this may affect their overall satisfaction with ECMWF support services, two surveys were conducted in 2022: one for ECMWF commercial licensees and the other for users of the EU-funded Copernicus Atmosphere Monitoring Service (CAMS) and the Copernicus Climate Change Service (C3S), which are both implemented by ECMWF. Both surveys were open for a two-week period in May–June 2022.

Outline of the surveys

ECMWF commercial licensing covers real-time data delivery, archive access and web data products for commercial customers, but also licences covering the distribution of data to national meteorological and hydrological services (NMHSs) outside ECMWF’s Member and Co-operating States and to research projects. In the survey for commercial licensees, over 380 existing licence holders spanning all licence types were contacted and asked seven core questions. These questions focused primarily on the service channels new and existing licensees were using for purchasing data, what they thought of documentation related to their licence (such as the Products Requirements Catalogue and ECMWF Data Store documentation), and what support channels they were using for general queries and issues. For the CAMS and C3S survey, over 66,500 distinct users were contacted, all of whom had interacted with the Copernicus Climate and Atmosphere Data Stores (CDS and ADS) and/or support channels (Knowledge Base, Forum, Support Portal) in the previous 15 months. A set of five core questions, primarily focused on the support channels, were put to users to collect their reaction and satisfaction. Both surveys asked for feedback regarding any changes they had perceived over the last 12 months, what changes they would like to see, and any general comments to help improve support services.

The response rate was 34 of over 380 commercial licensees (about 9%) and almost 1,300 of over 66,500 CAMS and C3S users (about 2%).

Main results and recommendations

The overall result was positive for both surveys, with a high amount of praise and constructive feedback for the support services, paving the way for further improvement. Significant changes (such as the retirement of support email addresses) were noticed by some but more crucially were not perceived as deterrents from getting support. Following analysis of the results, a number of recommendations have been derived. These recommendations will help refine the shape of the Support Services, applications and various support channels to better serve their users.

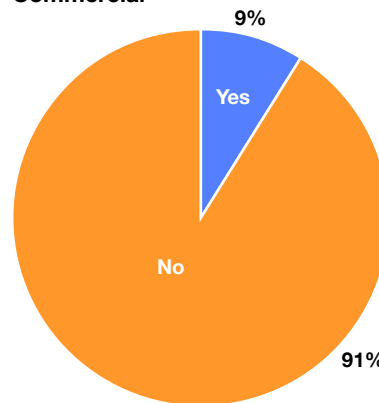
For ECMWF commercial licensees:

- Reinforce the use of the ECMWF Support Portal as the primary method of reaching out to the Data Support Team dedicated to commercial licensees.
- Improve the ‘ease of use’ of applications and provide links to help discover documentation and examples.
- Enhance the availability of services and applications to different licensees via a ‘Welcome Pack’. Welcome Packs also to include troubleshooting material to encourage users to resolve common issues themselves.

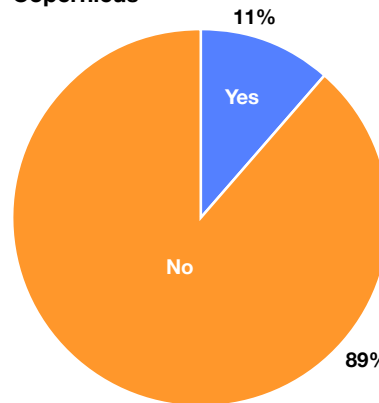
For CAMS and C3S users:

- Prioritise improving the Knowledge Base, in particular with enhanced accessibility for novices by introducing levels of documentation.
- Improve Forum functionality for greater usability (dedicated platform and service promotion).
- Implement and promote the Virtual Assistant on the CDS to facilitate

Commercial



Copernicus



Awareness of changes in support services.

Commercial licensees and CAMS and C3S users were asked whether they had noticed any changes in support services over the previous 12 months. A small percentage said they were aware.

smart integrated support journeys.

- Encourage synergies between Training and Support services to improve accessibility of training materials through support.

Conclusion

After the surveys, there is a better understanding of the impact of the changes that have been implemented over the past few years on users and their satisfaction. In future, a communication campaign could help yield a higher response rate from users contacted. Among the survey responses there were many useful comments, which will help the services evolve.

OpenIFS user meeting focuses on atmospheric composition

Marcus O. Köhler, Adrian A. Hill (both ECMWF), Mario Acosta (BSC)

OpenIFS aims to provide and support versions of ECMWF's operational Integrated Forecasting System (IFS) for research, education and training. An important aspect of the OpenIFS activity is active engagement with the model's user community. To support this, OpenIFS staff at ECMWF organise user meetings, which take place every couple of years and which are typically hosted at an institution in an ECMWF Member State. The 6th OpenIFS User Meeting took place from 22 to 26 May 2023 and was hosted at the Barcelona Supercomputing Center (BSC) in Spain. It focused on atmospheric composition and its role in numerical weather prediction (NWP).

Role of user meetings

The purpose of OpenIFS user meetings is to facilitate networking between model users and to enable sharing of their experiences in using OpenIFS. During the meeting, participants demonstrate their research activities with OpenIFS through oral and poster presentations. The meetings are also an opportunity for ECMWF to showcase the latest developments with OpenIFS. This is done through guided exercises in the form of computer practicals, which

accompany the scientific theme of the speaker programme. As such, OpenIFS meetings are not training courses. Instead they are science-focused workshops for the user community, which include practical elements that often give early access to pre-releases of forthcoming versions of OpenIFS software. OpenIFS staff also benefit from these events by receiving first-hand feedback from model users about recent OpenIFS developments.

The May 2023 meeting

The BSC Earth Sciences Department is home to a large and wide-ranging group of researchers working actively with OpenIFS. There were 42 meeting participants, who came from many ECMWF Member States, and also from further afield, such as from China and South Korea. The meeting began with Stephen English, Deputy Director of Research at ECMWF, and Francisco Doblas Reyes, Director of Earth Sciences at BSC, welcoming all participants to the meeting, before an introductory day about OpenIFS for new model users. During the remainder of the week, the meeting focused on atmospheric composition and its role in NWP, with a combination of invited and

contributed presentations. On Tuesday, the focus was on interactions between composition and meteorology in general, and gas-phase chemistry in particular. On Wednesday, the speakers explored the role of aerosol processes and recent improvements in their representation within NWP models. On Tuesday and Wednesday afternoon, the participants worked through atmospheric-composition-themed computer practicals on the European Weather Cloud. These practicals introduced the new OpenIFS/AC model configuration, which was developed at the Royal Netherlands Meteorological Institute (KNMI). They focused on the new capability of simulating atmospheric composition, as well as demonstrating the visualisation of model outputs with the Metview software package. On Thursday, the programme widened the scope to consider impacts of composition on longer, climate-relevant timescales, which included presentations from the EC-Earth community. The meeting concluded on Friday with a focus on topics about future developments. These included a preview of the next release, OpenIFS 48r1, and on the role of machine learning applications in NWP and their potential role in simulating atmospheric composition.



Group photo. Participants of the 6th OpenIFS User Meeting at the Barcelona Supercomputing Center. (Credit: BSC)

Engaging discussions

This successful meeting was attended both by long-standing OpenIFS users, who in some cases could provide a user perspective reaching back to when OpenIFS started, and by many new users, who are now ready to adopt the model in their forthcoming work. We received a range of excellent and stimulating oral presentations, with invited speakers from ECMWF, BSC, KNMI, the Finnish Meteorological Institute (FMI), the Swedish

Meteorological and Hydrological Institute (SMHI), the French company HYGEOS, and the UK Met Office. The talks from the research community demonstrated impressively the breadth of research applications for which OpenIFS is used, both in meteorology and NWP as well as increasingly in the interactions between atmospheric composition and NWP, and also in climate studies. The meeting produced very engaging discussions, both on research topics and on current and future model developments.

The forthcoming OpenIFS model upgrade to the operational IFS Cycle 48r1 received strong positive feedback from participants, as did the availability of the OpenIFS Data Hub to generate data for experiments. We would like to express our gratitude to all meeting participants in Barcelona, including remote speakers, computational support staff, and the entire organising team for contributing to a memorable and productive OpenIFS user meeting.

How well did we forecast the winter 2022/23?

Antje Weisheimer

Seasonal forecasts of the winter 2022/23 in Europe were anticipated with great interest, beyond pure scientific curiosity, due to their relevance to energy security concerns across the continent in relation to the war in Ukraine. Here we review how ECMWF's seasonal forecasting system SEAS5 performed and discuss the role of the El Niño–Southern Oscillation (ENSO) as a potential driver of large-scale circulation anomalies in the Euro-Atlantic area.

The largest source of predictability on seasonal timescales comes from the state of the tropical Pacific Ocean, with ENSO leading to teleconnections in remote parts of the world. Sea-surface temperatures (SSTs) in the central equatorial Pacific continued to be anomalously cold, resulting in the third consecutive La Niña winter. Such triple-dip cold La Niña events are rare, with only three previous occurrences since 1950.

Sea-surface temperature anomalies

The global seasonal mean (December to February, DJF) SST anomaly map from the ERA5 reanalysis (top-left panel in the figure) shows the cold La Niña conditions together with a warm tropical Atlantic and cold tropical Indian Ocean. The extratropical SSTs in the northern hemisphere were mainly warmer than during the climatological period 1993–2016. SEAS5 provided a good forecast of this situation, as can be seen in the top-right panel of the

figure, showing the ensemble-mean forecast anomaly. The large-scale structures in both the tropics and extra-tropics were well reproduced with some differences in the spatial extent or magnitude of the anomalies.

Near-surface temperature anomalies

Near-surface temperature anomalies over the oceans, which are strongly linked to the underlying SSTs, were well reproduced in the forecast (see the middle panels of the figure). The observed situation over land was characterised by warmer than average temperatures over Europe, with maximum anomalies over the eastern parts. The seasonal forecasts predicted the temperature anomalies for western and central Europe well but overestimated the statistical significance and the extent of the warm signal from eastern Europe through to Siberia. North America saw a northwest–southeast dipole structure with (non-significant) cold conditions in the northwest and significant positive anomalies over the east coast of the US. SEAS5 predicted a strong north–south difference with significant warm anomalies over most parts of the US. The observed far-eastern cold anomalies over Asia were strong in magnitude and significant compared to the level of interannual variability. SEAS5 missed the cold signal there. Temperature forecasts over South America verified very well, as did those over large parts of Africa. The significant cold conditions in the

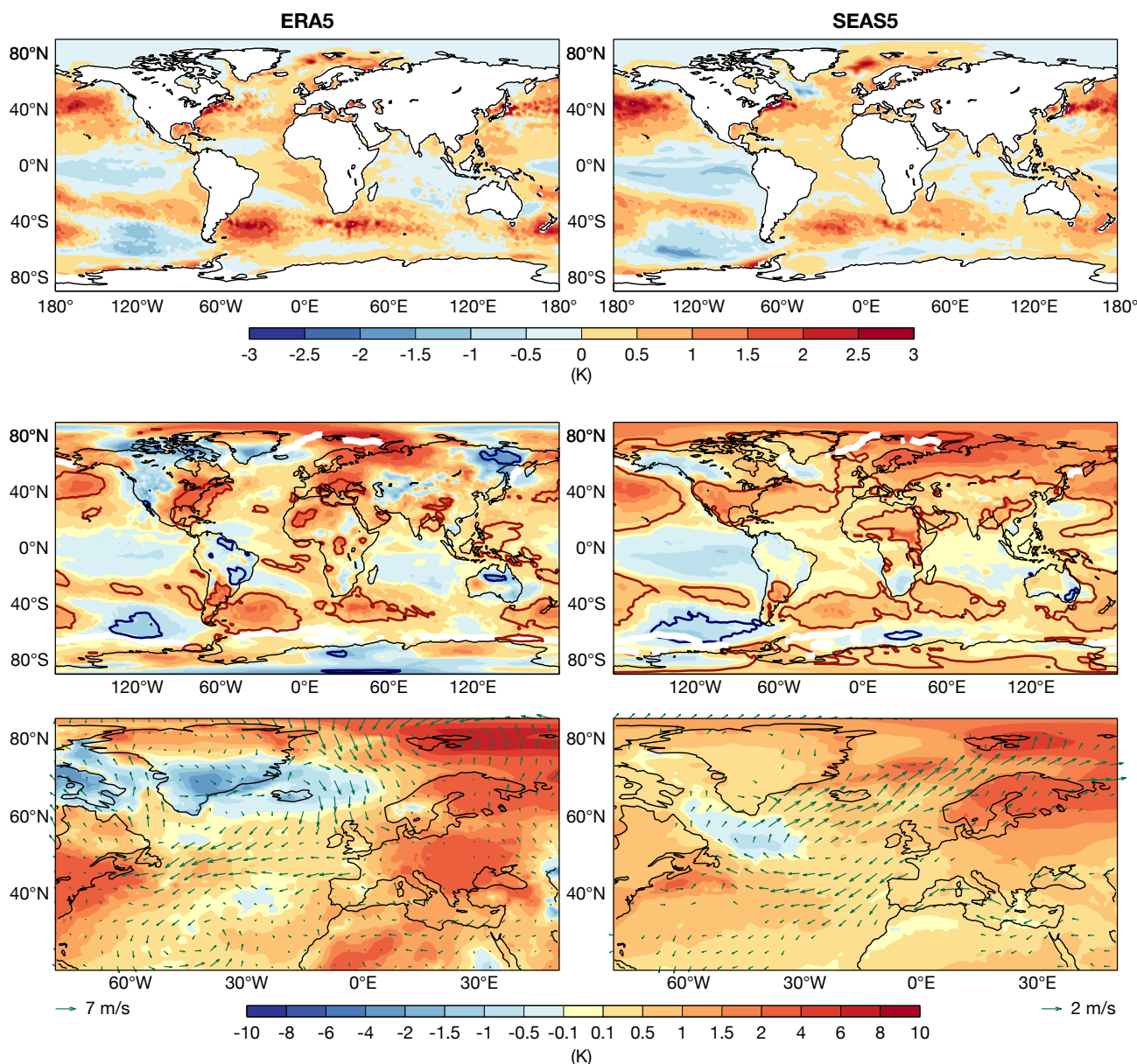
north-eastern parts of Australia were only partially reproduced with SEAS5.

The North Atlantic and Europe

A closer look into the conditions over the North Atlantic and Europe is provided in the two bottom panels of the figure, which also show 10-metre wind anomalies. While the overall warm signal over land was well predicted, the circulation showed several differences in the forecast compared with the reanalysis. Iceland, the Denmark Strait, and southern parts of Greenland experienced cold anomalies. This was due to anticyclonic conditions from the surface to the mid-troposphere that resulted in a negative observed North Atlantic Oscillation (NAO) index (not shown). The circulation around the high-pressure ridge brought a northerly wind anomaly component into Europe, especially over the North Sea, and led to weaker westerlies west of Europe and over the central North Atlantic than usual. The forecast missed the cold high-pressure centre over Greenland and instead produced more of a classical positive NAO pattern. This led to errors in the near-surface wind at Europe's northern and western coastlines.

Reasons for the North Atlantic circulation

Which physical driving mechanism could have influenced the circulation over the North Atlantic during the winter? The cold phase of ENSO is



Reanalysis and SEAS5 seasonal forecasts for December–January–February 2022/23. The top two panels show sea-surface temperature anomalies. The middle panels show global 2-metre temperature anomalies – red/blue contour lines indicate the local +/- 1.5 standard deviation level of the anomaly and the white contour line shows the sea-ice edge. The bottom panels show 2-metre temperature and 10-metre wind anomalies over the Euro-Atlantic region. All anomalies are computed with respect to the corresponding 1993–2016 climatological period. SEAS5 anomalies refer to ensemble means for forecasts started on 1 November 2022.

known to have weak statistical teleconnections into the North Atlantic and Europe. These tend to lead to high pressure anomalies in November and December and to a zonal positive NAO structure in January and February. The circulation during the 2022/23 winter, however, underwent substantial month-to-month variability (not shown), which did not match the canonical La Niña teleconnection structures. On the other hand, the SEAS5 forecast model, while failing to show a consistent classical surface pressure ENSO response during November and December, did predict

the expected ENSO-related zonal flow signal for late winter during January and February.

Given the correct ENSO forcing in the model, the atmospheric circulation difference over the North Atlantic between observations and the seasonal prediction can be interpreted as follows: the unpredictable internal variability component dominated the observed realisation in ERA5, while the forced component of the ENSO signal manifested itself in the ensemble-mean seasonal forecast response in the second half of the winter.

C3S seasonal predictions

SEAS5 is one of the systems contributing to the multi-model ensemble of seasonal predictions provided by the EU’s Copernicus Climate Change Service (C3S) implemented by ECMWF. Other C3S seasonal forecast models showed broadly the same seasonal-mean temperature signals as SEAS5. However, there was less consensus in the forecasts of the atmospheric circulation for the Euro-Atlantic region. The considerable variety across the models was an indication that this aspect of the forecast was more difficult to predict.

ECMWF supports DWD ICON training

Ulrich Schättler, Daniel Rieger (both German Meteorological Service),
Bojan Kasic, Carsten Maass (both ECMWF)

The Numerical Model Training 2023 for the ICON model took place from 27 to 31 March at the headquarters of the German Meteorological Service (DWD) in Offenbach, Germany, using resources on ECMWF's Atos high-performance computing facility (HPCF).

ICON training

For more than 20 years, the Department for Numerical Modelling and Analysis of DWD has organised training courses for using its numerical weather prediction (NWP) models. It started as a two-hour add-on of the User Seminar (now called ICCARUS) and soon extended to a full-week event with theoretical lessons on model components and practical exercises to install and run the models. Since 2019, the courses have only covered the ICON model, which can run in global and limited-area mode. At DWD, ICON has replaced all regional applications formerly operated with the COSMO model. All partners still running COSMO will migrate to ICON soon.

ICON applications range from NWP and regional climate simulations (CLM – Climate Limited-Area Model) to the prediction of trace substance dispersion with ICON-ART. Therefore, ICON users include national meteorological services, universities and research institutions, which form the target groups of the training course. After four years without any face-to-face training due to COVID, high demand for this course was expected, and three parallel exercise groups were planned from an early stage: NWP for universities (Academia), regional climate simulations (CLM), and NWP for national meteorological services (MetService).

Using ECMWF's Atos HPCF

As the number of trainees exceeded DWD's training resources, we contacted ECMWF User Services several months ahead of the event. We asked for the possibility to run practical exercises on ECMWF's Atos HPCF, thus allowing the MetService training group to run parallel jobs across multiple nodes. Meanwhile, the German Climate Computing Centre (DKRZ) was asked to provide computing resources for the Academia and CLM parts of the course. Both ECMWF and DKRZ agreed to make their HPCFs available.

Participants were asked to bring their own laptops. Individual trainee accounts were created by DWD. They were set up for time-based one-time password (TOTP) login and customised with the help of oathtool. Access to the Atos HPCF was realised via the Virtual Desktop Infrastructure (VDI), which provides a Linux desktop running in ECMWF's data centre. This allowed participants to compile programs, run and control jobs, and visualise the results of their ICON runs just through a web browser. To log in, most participants were using a TOTP generator on their smartphones.

A total of 71 participants from 19 countries took part in the training. They included representatives from nine African national meteorological and hydrological services, who could attend thanks to support by the World Meteorological Organization (WMO).

For the first time, tailored exercises with the ICON model were offered to the MetService group. These

exercises and corresponding materials had been developed by a group of COSMO scientists: U. Schättler and J.-N. Weiß (DWD); S. Dinicila, S. Gabrian and R. Dumitrache (Romanian National Meteorological Administration); W. Interewicz and D. Wojcek (Polish Institute of Meteorology and Water Management); and A. Shtivelman (Israel Meteorological Service). Several online meetings were held in the weeks before the course to coordinate and discuss the necessary work. Colleagues from Romania and DWD were present in Offenbach to guide the participants through the exercises.

The first task was to generate a grid and external parameters for their own model area using DWD's grid generator web service. The pre-processing step (interpolation of global ICON data to a regional grid) and the execution of an ICON-LAM simulation were then performed by all trainees on a provided grid under the guidance of the tutors. These steps then had to be transferred to the self-generated grid in the individual participants' target areas.

The provided grid was limited in size so that a 48-hour forecast could be run in five minutes on one Atos node. Forecasts with self-generated grids could run on up to three nodes. To ensure a quick job turnaround, ECMWF reserved a set of Atos nodes for this activity. Exercises to visualise the model results rounded off the practical learning content.

During the last afternoon, Axel Bonet and Iain Russell (ECMWF) gave online presentations and a tutorial on ECMWF's workflow package ecFlow,



Group photo.

Participants of the Numerical Model Training 2023.

used to run a large number of programs with dependencies on each other and on time in a controlled environment. In the Jupyter-Notebook-based tutorial, ecFlow was used to automate the execution of all steps that were run manually during the

training week. This is necessary for the operational implementation of an NWP suite at a meteorological service.

DWD and the COSMO partners would like to express sincere thanks to ECMWF and the DKRZ for the

opportunity to use their HPCFs. Special thanks go to ECMWF User Services for their extraordinary assistance during planning and conducting the exercises. Also, the presentations and tutorial on ecFlow were highly appreciated.

Major upgrade of CAMS forecasts of atmospheric composition

Johannes Flemming

The operational forecasting system for global atmospheric composition of the EU's Copernicus Atmosphere Monitoring Service (CAMS), implemented by ECMWF, has been substantially extended with the upgrade to Cycle 48r1 of the Integrated Forecasting System (IFS) on 27 June 2023.

The most important innovations are:

- the simulation of stratospheric chemistry with the BASCOE scheme
- the addition of secondary organic aerosols and new tropospheric species
- improved treatment of sectorial emissions
- assimilation of carbon monoxide retrievals from the Sentinel-5P satellite.

Stratospheric chemistry in the IFS

IFS components concerning atmospheric composition (IFS-COMPO), which are activated in global CAMS forecasts with the IFS, are developed in collaboration with European research institutes and national weather services. Several schemes for both tropospheric and stratospheric chemistry are implemented in the IFS. They include the Belgian Assimilation System for Chemical Observations (BASCOE) and the Carbon Bond Mechanism 5 (CB05).

The development of stratospheric BASCOE chemistry in the IFS had reached sufficient maturity to be applied operationally in Cycle 48r1, in

combination with the tropospheric CB05 scheme. Important steps were updates to the photolysis calculation in BASCOE and the introduction of the advection of chemical families to mitigate long-term trends caused by the lack of mass-conservation in the IFS. Prior to Cycle 48r1, linear parametrizations of stratospheric ozone chemistry, which are still applied in IFS numerical weather prediction (NWP) applications, were used in the operational CAMS forecast in combination with the CB05 scheme.

The CB05-BASCOE scheme makes it possible to fully represent chemistry throughout the atmosphere in the IFS in the operational CAMS forecast of Cycle 48r1 as well as in the upcoming production of a new version of the CAMS reanalysis of atmospheric composition. This means that CAMS will be able to forecast and monitor chemical species that control the formation of the ozone hole caused by long-lived ozone depleting substances, such as chlorofluorocarbons (CFCs) and hydrochlorofluorocarbons (HCFCs) and their short-lived products that cause the actual ozone destruction (see the figure). Processes such as the production of stratospheric water vapor by oxidation of methane, which is approximated by a parametrization in NWP applications of the IFS, can also be accounted for more realistically. Finally, the introduction of stratospheric chemistry in the IFS opens new opportunities for the data assimilation of satellite observations of stratospheric trace gases, such as bromine monoxide

(BrO), chlorine monoxide (ClO) or nitrogen dioxide (NO₂).

Secondary organic aerosols and new tropospheric species

Secondary organic aerosols (SOA) are a substantial fraction of observed particulate matter concentrations. Up to Cycle 47r3, SOAs were not simulated in the IFS, and simplified assumptions were made to treat them as part of primary organic matter aerosol. With Cycle 48r1, two SOA species, originating from anthropogenic or biogenic condensable organic precursor gases, were introduced in the AER aerosol scheme of IFS-COMPO. While this approach is still simple considering the complexity of SOA formation, it is an important first step to better represent SOAs and to account for transport during the time it takes to convert gaseous precursor emissions into SOA.

The tropospheric chemistry scheme based on CB05 in Cycle 48r1 has been extended to include the chemical species glyoxal and hydrogen cyanide (HCN). Tropospheric glyoxal concentrations can be retrieved from satellite instruments such as TROPOMI on Sentinel-5P and the CAMS forecast can provide glyoxal data as prior information to these retrievals. HCN is an important tracer of biomass burning and can also be observed from space. Increased concentrations of HCN can contaminate infrared (IR) radiances from satellite instruments, and operational HCN forecasts may contribute to the quality control of assimilated IR radiances in NWP applications.

Improved representation of emissions

The emission processing for the CAMS global forecasting system has recently undergone a major restructuring. As a consequence, emissions for individual emission sectors, and not just the total emission, can be ingested in the IFS to enable the sector-specific application of diurnal cycles and injection heights. For example, emissions from industry and power generation, which are released by chimneys, are now emitted in a specific height range above the surface, whereas emissions from transport are emitted at the surface following a predefined diurnal profile. This update has contributed to improved forecasts of surface concentration of air pollutants in Europe, China and North America. Cycle 48r1 also uses more recent versions of anthropogenic and biogenic CAMS-GLOB (ANT5.3, BIO-3.1) inventory datasets.

Emissions of desert dust, which are calculated online in the IFS based on turbulent wind fields and soil properties, as well as the removal of dust by deposition, have been greatly revised in Cycle 48r1. The dust burden in Cycle 48r1 is about twice as high as the one in Cycle 47r3, and more weight was given to the super-coarse dust bin, which is in better agreement with observations.

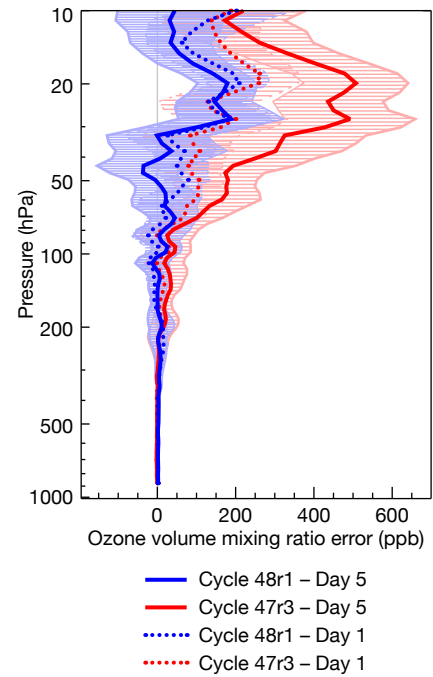
Assimilated observations

The activation of the assimilation of new satellite retrievals of atmospheric composition does not always follow the cycle upgrade timeline, but Cycle 48r1 brought the start of the assimilation of total carbon monoxide (CO) retrievals from the TROPOMI instrument in addition to the ongoing assimilation of CO retrievals from the IASI and MOPITT instruments. This update led to a better forecast of long-range transport from intensive wildfires in Canada in June 2023.

Impact and way forward

CAMS forecasts are verified using independent observations from a wide range of different networks by external partners, led by the Royal Netherlands Meteorological Institute (KNMI). The evaluation of the Cycle 48r1 experimental forecasting system concluded that most of the forecast parameters, in particular carbon monoxide, Aerosol Optical Depth, ozone and nitrogen dioxide showed improved forecast accuracy.

The IFS-COMPO updates for Cycle 48r1 also provide opportunities for the introduction of more refined modelling approaches and a wider range of applications of the forecast, in particular for stratospheric trace gases and aerosols. Finally, it should be mentioned that a comprehensive documentation of the atmospheric composition aspect in the IFS has been compiled for the first time. This



CAMS ozone forecast errors. Error of the CAMS ozone forecast for day 1 and day 5 of Cycle 48r1 (blue) and Cycle 47r3 (red) against five ozone sondes over Antarctica in October 2022 during the ozone hole event. The ozone forecasts for day 1 are similar as they are initialised from the respective ozone analysis. The forecast errors for day 5 in the stratosphere (50–10 hPa) are much smaller in Cycle 48r1 than in Cycle 47r3. The horizontal lines show variability within ± 1 standard deviation.

has been published as part of the IFS documentation relating to Cycle 48r1 (<https://www.ecmwf.int/en/publications/ifs-documentation>).

Increased use of surface observations

Cristina Prates, Volkan Firat, Umberto Modigliani, Bruce Ingleby, Mohamed Dahoui, Cristiano Zanna, Ersagun Kuşcu, Thomas Haiden

In-situ observations, and in particular surface land observations, play an important role in numerical weather prediction (NWP) models. At ECMWF, these land observations are used in the atmospheric data assimilation system (4D-Var) as well as in the Land Data Assimilation System (LDAS). Over land, SYNOP weather reports from ground stations are exchanged via the World Meteorological Organization (WMO) Global Telecommunication System (GTS). They are the primary

source of measurements for near-surface atmospheric parameters, such as surface pressure, 2-metre temperature, 10-metre wind, 2-metre humidity, and snow depth. For example, ECMWF's atmospheric 4D-Var currently assimilates surface pressure and daytime relative humidity, and there is work in progress towards assimilating 2-metre temperature and humidity (both day and night). Good coverage and better use of these near-surface observations contribute to a more accurate estimate

of the initial atmospheric state (analysis). This in turn leads to a better forecast, particularly for near-surface parameters, which are key for many forecast users.

In recent years, ECMWF has made an effort to acquire and use additional surface observations not being distributed on the GTS. ECMWF's support for the WMO-initiated South-East European Multi-Hazard Early Warning Advisory System (SEE-MHEWS-A) project represented an

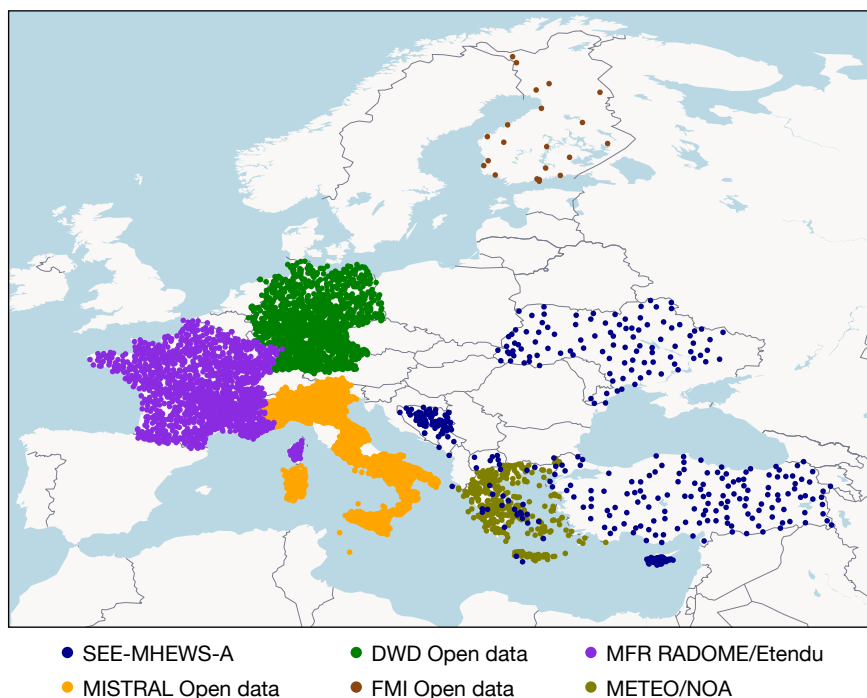
important milestone for the development of custom acquisition and pre-processing workflows enabling the use of additional surface observations.

Additional surface observations

Some tools were developed within the Scalable Acquisition and Pre-Processing (SAPP) system at ECMWF to facilitate the acquisition of SEE-MHEWS-A SYNOP data that could not be provided in the standard BUFR format. This includes handling local and national identifiers for stations not yet registered in the WMO's repository of metadata for surface-based observing stations, OSCAR/Surface. These developments also made it possible to acquire and use observations from the Forecasting & Monitoring of Weather Related Natural Disasters unit of the National Observatory of Athens (METEO/NOA) and Météo-France's extended network, including the RADOME network (MFR RADOME/Etendu).

Customised workflows were also implemented to enable the acquisition of open data from the Meteo Italian Supercomputing Portal (MISTRAL) and open surface observations from the German National Meteorological Service (DWD) and the Finnish Meteorological Institute (FMI). The first figure shows the locations of stations from which data were acquired from the sources mentioned.

Major developments made in handling WMO Integrated Global Observing System (WIGOS) Station Identifiers (WSI) were crucial for enabling the use of surface observations from newly registered observing stations. WSI processing was introduced in ECMWF's Integrated Forecasting System (IFS Cycle 47r1). The entire data handling software stack had to be adapted to account for the increased size of the new alphanumeric identifier compared to the five-digit numeric Traditional Station Identifiers (TSI). Thanks to these developments, it was possible to start processing additional data available on the GTS with only WSI. The second figure shows the locations of stations with WSI whose BUFR SYNOP data are acquired through the GTS. More than 450 of these stations have only WSI available, reporting either hourly (e.g. the ones from Colombia and Israel) or sub-hourly (e.g. the ones from Hungary and

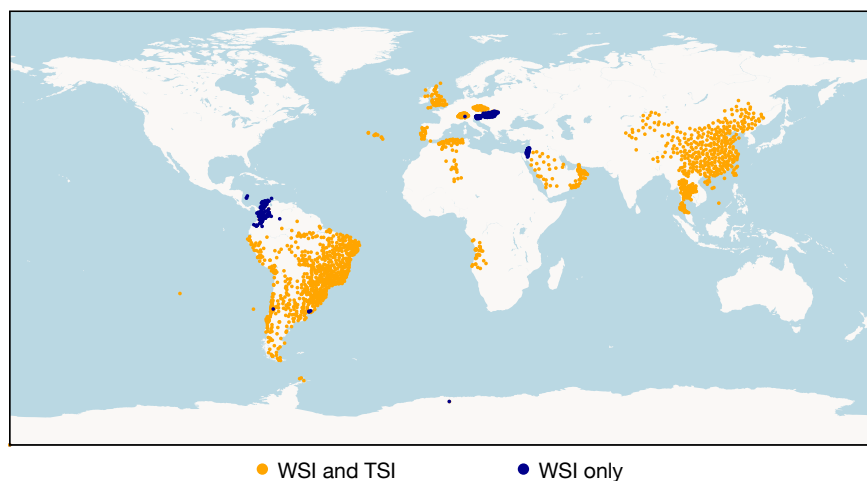


Use of more weather stations in Europe. Location of non-GTS stations from which SYNOP data were acquired at ECMWF over 30 days ending on 22 June 2023.

Slovenia). The rest of the stations have both WSI and TSI.

When batches of new stations are made available to 4D-Var by the acquisition system, their observations are not assimilated until their quality has been assessed based on statistics of their departures from a short-range forecast (the 'background'). This procedure is intended to ensure that new observations are safely introduced into the process of generating the initial conditions for a new forecast (the 'analysis') without the risk of introducing spurious features. Despite a huge

increase in the number of non-GTS stations, a large majority do not report surface pressure observations, which is one of the most important atmospheric quantities for global models. Of those that do, a large proportion are providing observations of a quality deemed good enough to be assimilated. The data selection is reviewed periodically, and good-quality stations will be added. On the other hand, most of the non-GTS stations report 2-metre temperature observations, which at the moment are only used in LDAS. However, only a small percentage is actually used in



WSI and TSI stations. Location of GTS available stations having WSI and TSI (orange) and only WSI (blue) from which BUFR SYNOP data were acquired at ECMWF over 30 days ending on 22 June 2023.

LDAS due to poor observation quality, observation redundancy or elevation differences between the station and the corresponding model grid cell.

The way ahead

ECMWF has made an effort to acquire and process a wealth of surface data that had not been exploited for global NWP purposes before. As a result, some issues in the quality of the data have been exposed. However, this effort will eventually pay off if the quality issues that are preventing the use of some of the new observations are fixed.

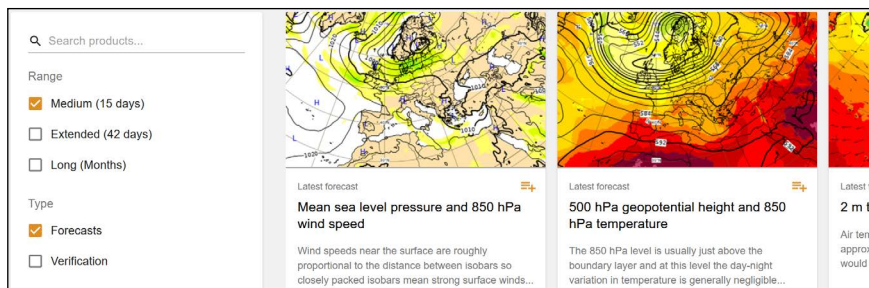
Enhancing observation capabilities is also a goal of the EU’s Destination Earth initiative (DestinE), in which ECMWF is involved. Observations are not just crucial for data assimilation but also very useful for forecast evaluation. This applies in particular to forecasts of extreme weather events, which is one of DestinE’s areas of interest. ECMWF is working together with several European national meteorological services and EUMETNET in the EU-funded RODEO project (<https://rodeo-project.eu>), which will support the provision of open access to public meteorological data.

In addition, the WMO Global Basic Observing Network (GBON), which went into effect on 1 January 2023, represents a cornerstone of the WMO’s strategy to secure observational data for critical global weather and climate applications. The GBON provisions for surface stations require the exchange of hourly observations. Many ECMWF Member and Co-operating States already provide hourly data, but where 3- or 6-hourly observations are currently exchanged, we encourage the exchange of hourly data to enable improved forecast products.

Open data community mailing list

Emma Pidduck (ECMWF), Hella Riede (DWD), Björn Reetz (DWD), Roope Tervo (EUMETSAT), Håvard Futsæter (MET Norway)

The weather and climate Open Data Mailing List is a valuable resource for anyone interested in staying informed about the latest developments in open data in the field of weather and climate in Europe. Created and moderated by colleagues from ECMWF, the German Meteorological Service (DWD), the Norwegian Meteorological Institute (MET Norway), and EUMETSAT, the mailing list provides a platform for all users to share updates on relevant open data, publications, applications, and conferences. The open data movement has been gaining momentum in recent years. It has become increasingly important to share information and insights to further advance the field, particularly in light of directives such as the EU Open Data Directive (including High Value Datasets) and more broadly the EU Open Science goal. The weather and climate community has an important role in the global conversation around open data. The data produced and shared by this community are crucial for understanding and responding to the impact of climate change on the



Open data on the ECMWF website. ECMWF offers a range of open charts and open data on its website.

environment and society. By openly sharing data, the community can accelerate progress and drive innovation.

The mailing list was inspired by the 2022 European Meteorological Society (EMS) conference session on ‘Open Data – data, application development, impact’, where co-convenors of the open data session realised that not everyone was aware of developments in other countries and that the community needed a simple and easy way to share this information centrally. The first edition of the mailing list was

launched in December 2022, with a later contribution from Environment and Climate Change Canada (ECCC) about its open data achievements in 2022.

By June 2023, the mailing list had already gained around 415 subscribers, and the hope is that members of the list will start to share more information. To subscribe, send a blank email to the open data community subscription list: open-data-community-subscribe@lists.ecmwf.int. You can also request sending content to the mailing list by emailing it to open-data-community@lists.ecmwf.int.

New observations April – June 2023

The following new observations have been activated in the operational ECMWF assimilation system during April – June 2023.

Observations	Main impact	Activation date
CO retrievals from Sentinel-5P	Carbon monoxide in the COMPO suite	27 June 2023 (Cycle 48r1)

IFS upgrade brings many improvements and unifies medium-range resolutions

Simon Lang, Dinand Schepers, Mark Rodwell

An upgrade of ECMWF's Integrated Forecasting System (IFS) was implemented on 27 June 2023. One highlight is a horizontal resolution increase of the medium-range ensemble (ENS) to TCo1279 (9 km), which brings it to the same resolution as the high-resolution forecast (HRES). In addition to upper-air score improvements, the new ENS especially improves the skill of surface variables, such as 2 m temperature and 10 m winds, and tropical cyclones. The number of ensemble members for the extended-range ensemble forecast has increased from 51 to 101 members, and it is now run daily instead of twice weekly. These configuration changes result in substantial improvements in skill and utility for users. IFS Cycle 48r1 also benefits from a multitude of improvements to the data assimilation system as well as the forecast model, including for example higher inner-loop resolution in the data assimilation system, the assimilation of surface-sensitive microwave imager channels over land and cold ocean surfaces, and a multi-layer snow scheme in the forecast model.

Forecast model

The horizontal resolution of medium-range ensemble forecasts is increased from TCo639 (18 km) to TCo1279 (9 km). The vertical resolution remains unchanged at 137 levels. This means that the ensemble is run at the same resolution as the single HRES forecast. The horizontal resolution increase leads to improvements in forecast skill for upper-air variables and especially for surface variables. In addition, extreme events such as tropical cyclones are better represented. One consequence is that the unperturbed ENS control forecast and the HRES forecast are meteorologically equivalent and equally skilful on average. However, they can diverge on a day-to-day basis due to small technical differences and the chaotic nature of the atmosphere. In future, one of these forecasts will be retired.

An example of the impact of the horizontal resolution increase can be seen in Figure 1 for the case of severe tropical cyclone Ilsa, which made landfall over Western Australia in April 2023. The Cycle 48r1 9 km ensemble forecasts initialised on 9 April (Figure 1a) predicted Ilsa's

intensity much better than the then operational 18 km ensemble forecast (Figure 1b). In addition, the 48r1 ensemble provided a more accurate track forecast.

Extended-range ensemble forecasts are now run daily instead of twice weekly, and the number of ensemble members has been increased from 51 to 101. Also, extended-range ensemble forecasts are no longer run as an extension to medium-range ensemble forecasts. Instead, they are run from initial time at a horizontal resolution of TCo319 (36 km) for the full forecast range, day 0 to 46. Hence, the horizontal resolution of the extended-range system is no longer higher for the first 15 days. Tests have confirmed that forecast scores for beyond that time do not deteriorate as a result of this change. The removal of the resolution truncation at day 15 will allow users to simplify their coding for products based on accumulated fields, such as precipitation. The extended-range forecasts are now archived in the new stream eefo, and the corresponding re-forecasts (from day 0) are now archived in the new stream eefh. The medium-range forecasts and re-forecasts remain in streams enfo and enfh, respectively. Initial condition and stochastic physics perturbations are introduced with different random numbers between medium-range and extended-range ensembles, which makes it possible to combine the two systems for forecast applications that would benefit from a larger ensemble size. In addition, the more frequent initialisation of extended-range forecasts raises the prospect of constructing lagged ensembles for this range. For more details on the extended-range upgrade, see Vitart et al. (2022).

A major change in the forecast model in Cycle 48r1 is from a single-layer to a multi-layer representation of snow in the surface scheme. The multi-layer snow scheme markedly improves the realism of the snow pack in the model and decreases the magnitude of analysis increments of snow depth. The impact on 2 m temperatures in snow-prone regions includes an improved daily cycle (Arduini et al., 2019), and there are reduced snow depth forecast errors (Figure 2).

Some of the IFS climate fields have been updated: the orography, the land–sea mask, lake depth and the glaciers mask. The improved climate fields increase the realism of inland water distribution and provide a more accurate surface skin temperature.

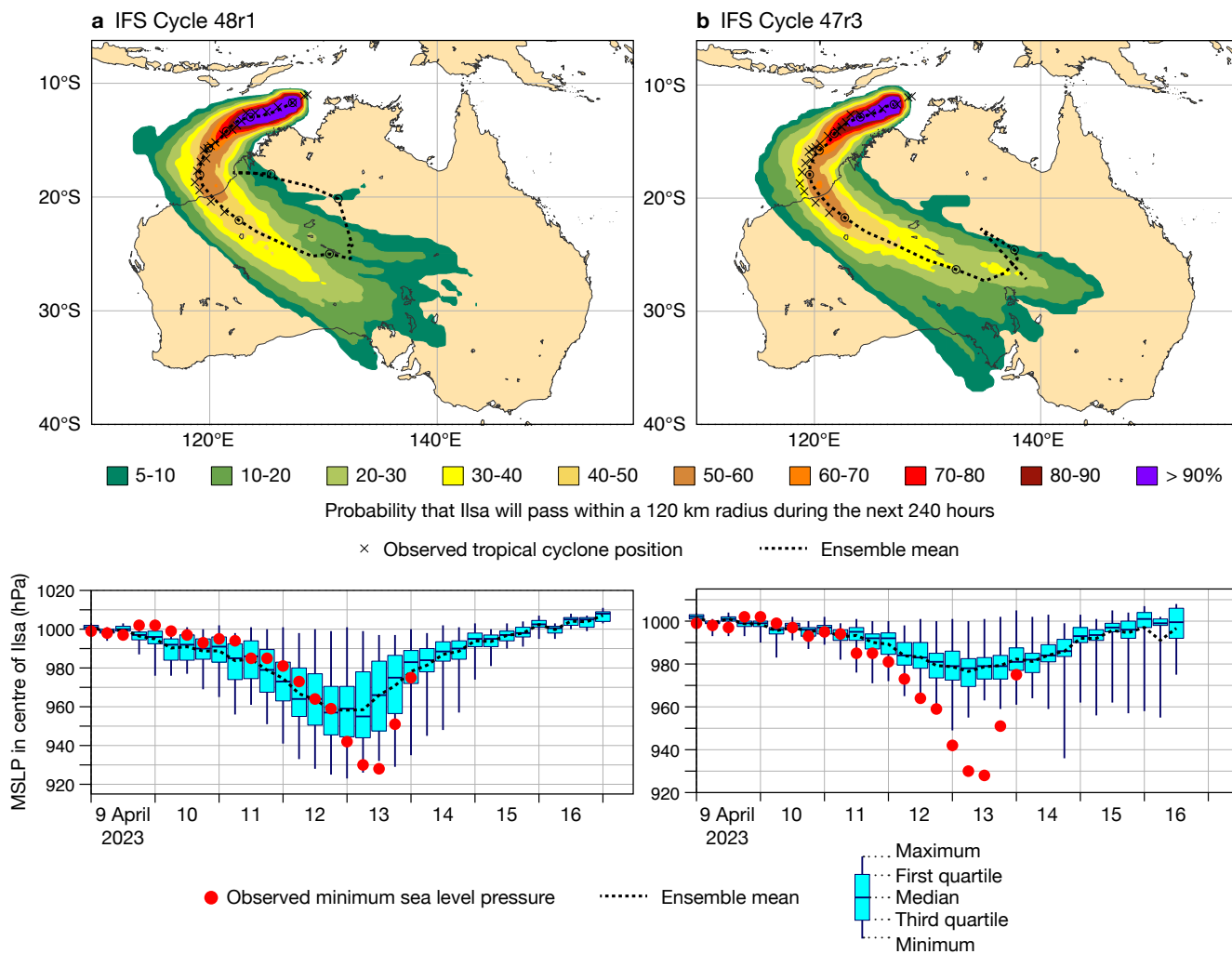


FIGURE 1 Tropical cyclone Ilsa, forecast from 9 April 2023, 00 UTC, in (a) the IFS Cycle 48r1 ensemble forecast with a resolution of 9 km, and (b) the IFS Cycle 47r3 ensemble forecast with a resolution of 18 km. Shown are the strike probability (top) and mean sea level pressure (MSLP) in the centre of Ilsa (bottom).

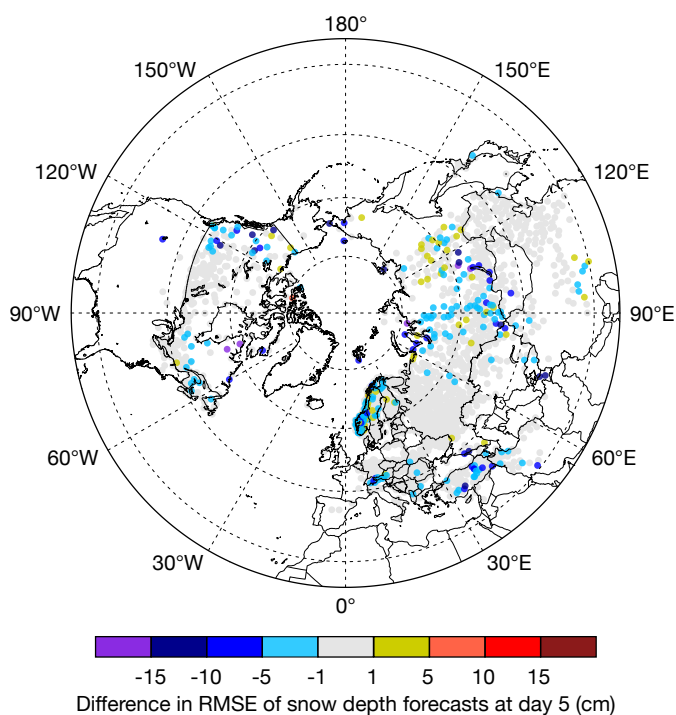


FIGURE 2 The figure shows the difference between multi-layer and single-layer snow in the root-mean-square error (RMSE) of snow depth forecasts at day 5, compared with SYNOP weather station values in the 2019/20 winter. Blue colours indicate an improvement when multi-layer snow is used.

The parametrization of microphysical processes has been revised in Cycle 48r1 to allow supercooled drizzle drops to be formed and only to freeze if they come into contact with pre-existing ice or snow particles, or experience much colder temperatures. This allows the IFS to predict high-impact freezing drizzle events, where supercooled rain/drizzle drops freeze on impact at the surface and form a glaze of ice. Figure 3 shows an example case study on 19 December 2017 over Germany, where freezing drizzle was observed. The revised microphysical parametrization in Cycle 48r1 shows the occurrence of freezing drizzle in the area, while the operational forecast model at the time did not have this ability.

The partitioning of low-level orographic drag processes to the surface drag underwent a major change, which includes revisions of the subgrid orography fields and the orographic low-level flow blocking, and gravity wave drag parametrizations. The subgrid orography fields are now representative of orographic features with scales smaller than the effective orographic resolution of the forecast model (several times the grid length) rather than only scales smaller than the grid length (Kanehama et al., 2022). There is now a shallower sponge layer at the top of the forecast model, starting at 0.7 hPa instead of 10 hPa. This leads to a more realistic gravity-wave breaking level and thus an improved gravity-wave drag profile.

A new streamlined algorithm for the computation of semi-Lagrangian advection departure points is introduced in Cycle 48r1. It is based on a scheme that is more suitable for single precision calculations near the poles, resulting in a more compact and simplified code. It requires fewer iterations to achieve the same accuracy as the previous approach. Hence, the overall cost of the

scheme is reduced (Diamantakis & Váňa, 2022).

A new vertical Finite Element discretisation scheme (Vivoda et al., 2018) has been introduced in Cycle 48r1, which is applicable to both the hydrostatic and non-hydrostatic dynamical core options of the IFS and improves the conservation of the total air mass in single precision. To improve water and energy conservation properties in the IFS dynamics, global mass fixers have been activated for all moist species, including water vapour (Becker et al., 2022). Furthermore, some revisions to the saturation adjustment and ice fall speed have been made. Perturbations to the cloud saturation tendency have been removed from the Stochastically Perturbed Parametrization Tendencies scheme (SPPT) to avoid rare model instabilities. In addition to improving the underlying physical consistency of the IFS, the combined changes improve medium-range ensemble scores, especially in the tropics.

The physics–dynamics interface across the non-linear, tangent-linear and adjoint models has been made more consistent. As a result, the tangent-linear model now better approximates the full non-linear model.

Cycle 48r1 introduces the new Hybrid Linear Ozone (HLO) scheme. Some terms within the scheme are inferred from chemistry models, while others are inferred from multiple years of observationally constrained ozone reanalyses from the EU-funded Copernicus Atmosphere Monitoring Service (CAMS) implemented by ECMWF (Williams et al., 2021). The HLO scheme improves stratospheric wind forecasts. A semi-Lagrangian 2-grid-point vertical filter (SLVF) on temperature has been introduced above 100 hPa. This alleviates unphysical global-mean cooling in the stratosphere in the forecast

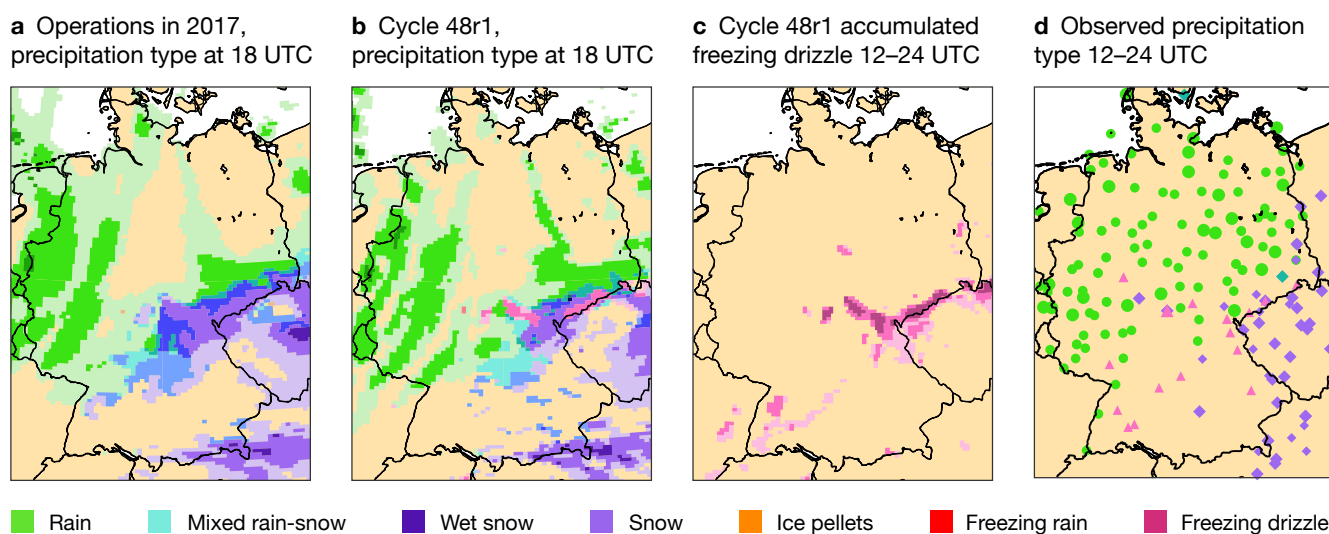
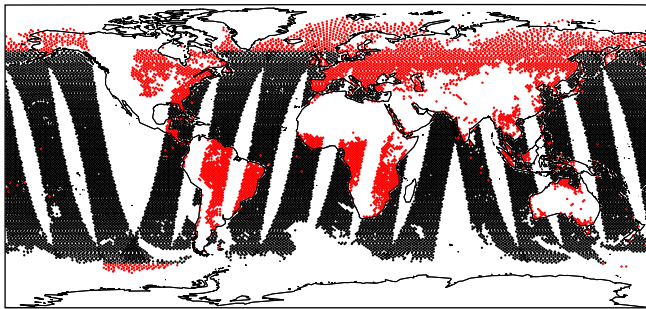


FIGURE 3 In this case from 19 December 2017, (a) no freezing drizzle was indicated in forecasts operational at the time, as in this short-range (18-hour) forecast, whereas (b) Cycle 48r1 predicts freezing drizzle. The locations of freezing drizzle in (c) 12–24 hour accumulations in Cycle 48r1 agrees well with (d) the observation reports over the same period. Shading indicates 0.02, 0.1 and 0.5 mm accumulated precipitation per hour in (a) and (b) and per 12 hours in (c).

a AMSR2



b MHS

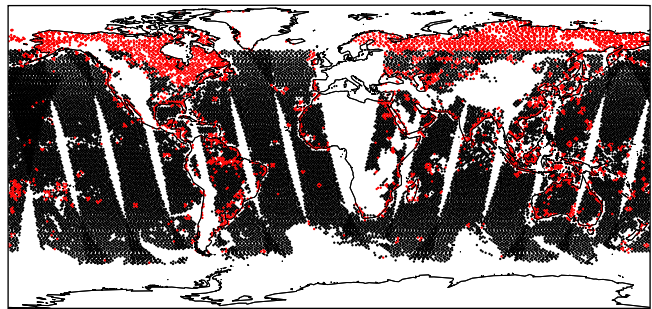


FIGURE 4 Example of the coverage of observations to be assimilated in Cycle 48r1 from (a) the Advanced Microwave Scanning Radiometer – 2 (AMSR2) in channel 11 (36.5 GHz v-polarised), and (b) the Microwave Humidity Sounder (MHS) on Metop-B in channel 5 (190.311 GHz), with black dots indicating data assimilated in Cycle 47r3 and red dots the data added in Cycle 48r1. Data are taken for the 00 UTC cycle on 20 June 2019.

model and improves the fit to GNSS-RO observations.

The wave model infrastructure has undergone wide-ranging optimisation, which will enable future high-resolution runs.

Data assimilation and observation usage

A major technical upgrade of the data assimilation system in Cycle 48r1 is the switch to the Object-Oriented Prediction System (OOPS). OOPS provides flexibility, which will facilitate the development of ECMWF's data assimilation capabilities in the future. In addition, it improves the scalability of the current system (English et al., 2017).

With Cycle 48r1, the Continuous Observation Processing Environment (COPE) has been introduced, which performs observation pre-processing incrementally shortly after observations are received. It is more scalable than the legacy observation processing system and will be able to scale to hundreds of billions of observations.

The resolution of the final inner loop of the 4D-Var data assimilation system is increased from TL399 (50 km) to TL511 (40 km), which enables a better fit to observations and improves forecast scores.

The radiative transfer model (Radiative Transfer for TOVS, RTTOV) used in the IFS has been upgraded to the latest version, RTTOV 13.0, bringing improved microwave radiative transfer as well as a major upgrade of cloud and precipitation optical properties (Geer et al., 2021; Barlakas et al., 2021).

In addition, the assimilation of satellite observations in the microwave spectral range has been improved by the implementation of a Lambertian representation of surface reflection over snow and ice (appearing uniformly bright from all directions of view), when previously a specular representation was used (incident radiation is reflected into a single outgoing

direction) (Bormann, 2022). There are also improvements through the activation of humidity-sensitive channels of the ATMS instrument over snow-covered areas in clear-sky conditions. Selected microwave channels and sensors now employ slant-path interpolation when assimilated in the all-sky system.

An important advancement in this cycle is the assimilation of microwave imager channels over snow-free land (excluding desert surfaces), enabled by an enhanced estimation of surface emissivity appropriate for all-sky assimilation (Figure 4a). Furthermore, improved sea-ice detection now allows assimilation of surface-sensitive microwave imager observations over land and ocean in high-latitude ranges (poleward of ± 60 degrees latitude). Other refinements include the addition of microwave humidity sounding radiances over land at high latitudes, as well as a better handling and increased usage of microwave sounding observation over mixed surfaces, involving land, water and sea ice, such as in coastal and lake regions (Geer et al., 2022) (Figure 4b). These changes are a key step towards an all-sky/all-surface use of microwave radiances.

The thinning of scatterometer observations has been significantly reduced so that the number of assimilated observations is strongly increased. This represents an important step towards a better analysis of low-level winds over sea areas, e.g. around tropical cyclones.

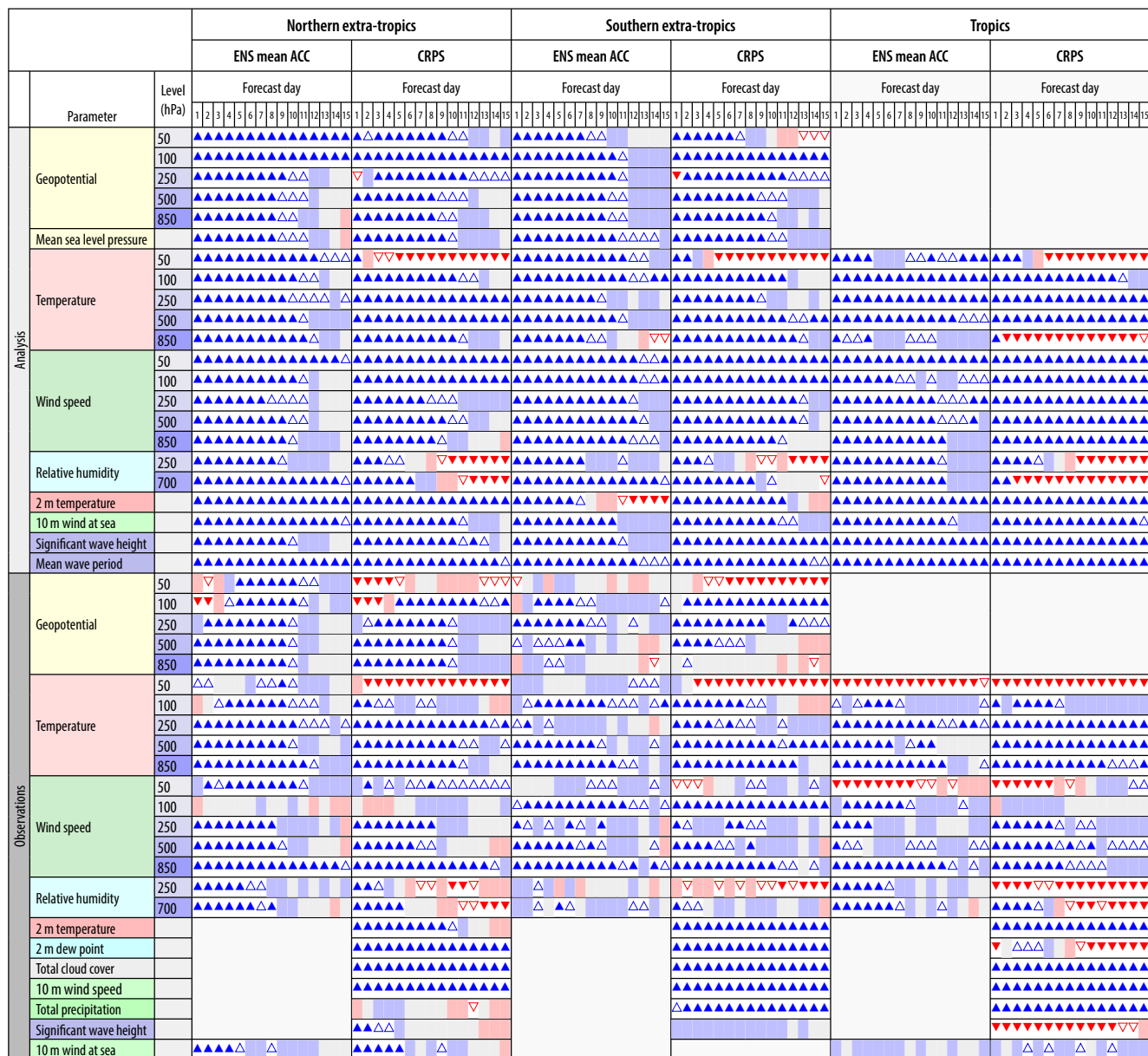
Additional developments have improved the assimilation of a suite of hyperspectral infrared sounders. Specifically, an improved trace gas detection scheme for identifying and rejecting soundings affected by excessive hydrogen cyanide concentrations, associated with forest fires, helps to reduce false alarms for IASI (Infrared Atmospheric Sounding Interferometer) and AIRS (Atmospheric Infrared Sounder). An upgraded aerosol-type classification now informs a channel-specific aerosol rejection algorithm over sea areas. Ozone-sensitive CRIS (Cross-track Infrared Sounder) channels are bias-

corrected taking into account the type of air-mass, bringing the approach into line with that used for similar channels on AIRS and IASI.

Impact on medium- and extended-range forecasts

The scorecard summarising the ENS score changes is shown in Figure 5. Most ENS scores of surface variables, such as 2 m temperature, 10 m wind and total

precipitation, are markedly improved, in the range of 2% to 6%. Most upper-air variables are improved as well, by around 1% to 3%. Stratospheric winds are improved, but some degradations of stratospheric temperatures due to increased biases can be observed. There are also pronounced improvements in scores over the Arctic and Antarctic, partly associated with the increased spread generated by the multi-layer snow scheme (not shown). The ensemble spread of upper-air variables (ensemble standard deviation, not shown) is reduced in the mid-



- Symbol legend:** for a given forecast step...
- ▲ 48r1 better than 47r3 statistically significant with 99.7% confidence
 - △ 48r1 better than 47r3 statistically significant with 95% confidence
 - 48r1 better than 47r3 statistically significant with 68% confidence
 - no significant difference between 47r3 and 48r1
 - 48r1 worse than 47r3 statistically significant with 68% confidence
 - ▽ 48r1 worse than 47r3 statistically significant with 95% confidence
 - ▼ 48r1 worse than 47r3 statistically significant with 99.7% confidence

FIGURE 5 This ENS scorecard compares IFS Cycle 48r1 with IFS Cycle 47r3 for the anomaly correlation coefficient (ACC) of the ensemble mean and the Continuous Ranked Probability Score (CRPS). It shows predominantly improvements (blue colours) and a few deteriorations (red colours). Results are verified by the respective analyses and observations at 00 and 12 UTC, based on about 550 forecast runs in the period June 2020 – April 2023.

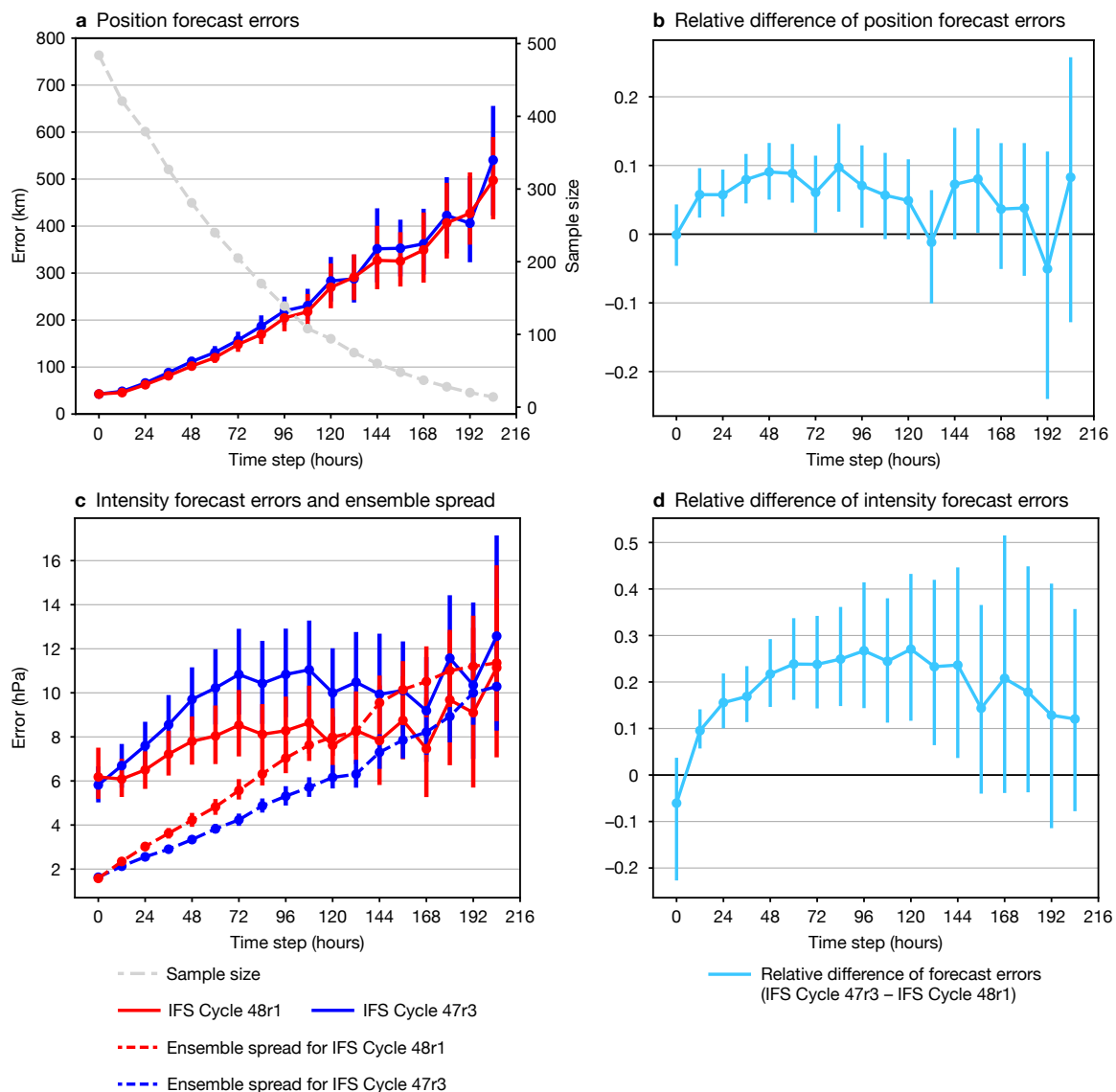


FIGURE 6 ENS tropical cyclone position and intensity forecast errors in IFS Cycle 48r1 compared to IFS Cycle 47r3, showing (a) position forecast errors of Cycle 48r1 and Cycle 47r3, (b) the relative difference of position forecast errors, with positive values showing improved forecast errors for Cycle 48r1, (c) intensity (central pressure) forecast errors (solid lines) and ensemble spread (dashed lines) of Cycle 48r1 and Cycle 47r3, and (d) the relative difference of intensity forecast errors, with positive values showing improved forecast errors for Cycle 48r1. The vertical error bars represent 95% confidence intervals.

latitudes (by around 1% to 2%) but mainly increased in the tropics (by around 2% to 3%), and the ensemble spread of surface variables is increased (by around 2% to 6%).

Cycle 48r1 improves ENS tropical cyclone track and intensity forecasts, with position errors reduced by up to 10% (Figure 6a,b) and core pressure errors reduced by around 20% (Figure 6c,d). The reduced track errors are mainly associated with a reduced slow-propagation bias of the forecast model. The intensity forecast is improved because the higher horizontal resolution allows for a better representation of the strong horizontal gradients associated with intense systems like tropical cyclones. This is also reflected in the strongly increased intensity spread of the ENS. The track spread, on the other hand, is very similar to that of the previous cycle (not shown).

The scores of the HRES forecast are summarised in Figure 7. These show clear overall improvements. Upper-air troposphere scores are improved by around 1% to 3% in the northern hemisphere and in the tropics. In line with the ENS, stratospheric winds are improved, but some degradations of stratospheric geopotential can be observed due to increased biases. These impacts are mainly related to the new HLO scheme. Upper-level Arctic and Antarctic scores are improved, in line with the ENS scores.

Surface winds in the tropics appear degraded when verified against ECMWF's analysis. This apparent degradation is caused by the large increase of scatterometer observations and the associated decorrelation of analysis and forecast errors. Verification

against observations does not show the degradation. HRES northern and southern hemisphere 2 m temperature scores also show some degradation, which comes from increased (more realistic) analysis and forecast activity generated by the multi-layer snow scheme. Tropical cyclone track and intensity forecast scores in HRES are very similar to those for the previous cycle.

The forecast model changes result in small improvements of the weekly mean extended-range scores. However, the increased ensemble size of the extended-range system, as well as the increased run frequency (daily instead of twice weekly), lead to substantial skill improvements (Vitart et al., 2022).

New products

There is an additional precipitation type (see WMO Table 4.201) to indicate the occurrence of freezing drizzle at the specified output time, as explained above (Figure 3). Cycle 48r1 also contains new parameter outputs for ‘most-frequent’ and ‘most-severe’ precipitation type in the last 1, 3 or 6 hours to complement the instantaneous precipitation type parameter.

Summary

IFS Cycle 48r1 brings many improvements and innovations for both the forecast model and the observation handling and data assimilation system. It introduces several important technical developments, like OOPS and COPE, and optimisation to future-proof the wave model. It also increases observation counts, for example of scatterometer observations, and it improves the data assimilation system, for example by the 4D-Var inner-loop resolution increase from TL399 to TL511, improving analysis accuracy. It has, among other things, a new multi-layer snow model for a more realistic representation of snow, the new Hybrid Linear Ozone scheme, and improvements to the dynamics which lead to markedly improved water and energy conservation properties of the forecast model. The combined data assimilation and model changes significantly improve forecast skill.

The extended-range system benefits from an increase in ensemble size, from 51 to 101 members. The daily initialisation of the extended-range system means that there are now up-to-date forecasts available at all times, instead of forecasts that can be several days old.

The horizontal resolution upgrade of the ENS from 18 to 9 km is a major step forward and brings it to the same resolution as the HRES forecast. In the future, the HRES forecast and the unperturbed control forecast of the ensemble will be merged. The resolution upgrade leads to marked improvements of upper-level scores and greatly improves forecast skill for surface variables, such as 2 m temperature and 10 m winds, and for extreme events, such as tropical cyclones.

Further reading

- Arduini, G., G. Balsamo, E. Dutra, J.J. Day, I. Sandu, S. Boussetta et al.**, 2019: Impact of a multi-layer snow scheme on near-surface weather forecasts. *Journal of Advances in Modeling Earth Systems*, **11**, 4687–4710. <https://doi.org/10.1029/2019MS001725>
- Barlakas, V., A.J. Geer & P. Eriksson**, 2021. Introducing hydrometeor orientation into all-sky microwave and submillimeter assimilation. *Atmospheric Measurement Techniques*, **14**(5), 3427–3447.
- Becker, T., T. Rackow, X. Pedruzo, I. Sandu, R. Forbes, M. Diamantakis et al.**, 2022: Fixing water and energy budget imbalances in the Integrated Forecasting System, *ECMWF Newsletter No. 172*, 14–15. <https://shorturl.at/BGOR6>
- Bormann, N.**, 2022. Accounting for Lambertian reflection in the assimilation of microwave sounding radiances over snow and sea-ice. *Quarterly Journal of the Royal Meteorological Society*, **148**(747), 2796–2813.
- Diamantakis, M. & F. Váña**, 2022: A new way of computing semi-Lagrangian advection in the IFS. *ECMWF Newsletter No. 173*. <https://doi.org/10.21957/md5f8jx27p>
- English, S., D. Salmond, M. Chrust, O. Marsden, A. Geer, E. Holm et al.**, 2017: Progress with running IFS 4D-Var under OOPS, *ECMWF Newsletter No. 153*, pp. 13–14. <https://www.ecmwf.int/en/newsletter/153/news/progress-running-ifs-4d-var-under-oops>
- Geer, A.J., K. Lonitz, D.I. Duncan & N. Bormann**, 2022: Improved surface treatment for all-sky microwave observations. *ECMWF Technical Memorandum No. 894*. <https://doi.org/10.21957/zi7q6hau>
- Geer, A.J., P. Bauer, K. Lonitz, V. Barlakas, P. Eriksson, J. Mendrok et al.**, 2021. Bulk hydrometeor optical properties for microwave and sub-millimetre radiative transfer in RTTOV-SCATT v13. 0. *Geoscientific Model Development*, **14**(12), 7497–7526.
- Kanehama, T., I. Sandu, A. Beljaars, A. van Niekerk, N. Wedi, S. Boussetta et al.**, 2022: Evaluation and optimization of orographic drag in the IFS, *ECMWF Technical Memorandum, No. 893*. <https://doi.org/10.21957/fps6gngqce>
- Vitart, F., M.A. Balmaseda, L. Ferranti & M. Fuentes**, 2022: The next extended-range configuration for IFS Cycle 48r1. *ECMWF Newsletter No. 173*. <https://doi.org/10.21957/fv6k37c49h>
- Vivoda, J., P. Smolikova, & J. Simarro**, 2018: Finite Elements Used in the Vertical Discretization of the Fully Compressible Core of the ALADIN System, *Monthly Weather Review*, **146**, <https://doi.org/10.1175/MWR-D-18-0043.1>
- Williams, R., R. Hogan, I. Polichtchouk, M. Hegglin, T. Stockdale & J. Flemming**, 2021: Evaluating the impact of prognostic ozone in IFS NWP forecasts. *ECMWF Technical Memorandum, No. 887*. <https://doi.org/10.21957/rakfo1qo3>

Interaction between polar and subtropical jet streams over Greece, 7–10 July 2022

Nicholas Prezerakos (former Director at the Hellenic National Meteorological Service)

In December 1973, R.M. Morris of the UK Met Office gave a lecture on ‘Synoptic Meteorology in the Mediterranean region’ at the Meteorological Office College in Reading. R.M. Morris had served for a long time as a senior forecaster in Cyprus gaining knowledge and skill on weather forecasting in the Mediterranean. Two subjects drew the author’s attention due to their importance for the configuration of weather systems over the Balkans, including Greece: a) the origin, structure and movement of depressions in northwest Africa and b) the possible interaction between polar jet streams (PJS) and subtropical jet streams (SJS).

The interaction between PJS and SJS is different in this region from the usual one. This well-known atmospheric circulation process contributes mainly to the rejuvenation of depressions whose origin is in the relatively low latitudes during northern hemisphere cold seasons, transforming those to vigorous extratropical systems. Many publications in the international meteorological literature have studied this phenomenon. Prezerakos et al. (2006) referred to most of these papers and stressed the important role of the interaction of the right-side entrance of a polar jet (PJ) streak with the left-side exit of a subtropical jet (SJ) one.

The author studied north African depressions, leading to three papers published in the *International Journal of Climatology*, revealing their baroclinic nature. The findings presented in these papers combined with the findings in the author’s earlier publications (Prezerakos et al., 1990; Prezerakos & Baltasis, 1977; and Prezerakos, 1985) to provide a comprehensive picture of north African depressions. In addition, many papers have been published in the international meteorological literature considering the subject mostly from the point of view of stratospheric intrusion of the Polar Vortex (PV). However, maxima of PV greater than the value of the dynamical tropopause should be examined more carefully before being characterised as ‘stratospheric intrusions’. Analyses of thermal (not dynamical) tropopause and maximum wind charts indicating the positions of its sharp folds should be considered, because the sources of vorticity are many and variable inside the troposphere.

In this article, we briefly present the main findings resulting from the study of atmospheric circulation conditions occurring when the SJS advances poleward far from its normal position over Crete in summer. We have discovered that, when the SJS shifts its position poleward far from Greece, or a sudden transformation of the atmospheric circulation index from high to low occurs, a large-scale anticyclone with tropical tropopause (mostly depicted as a sort of blocking with a SJ streak just at its north flank) is created, bringing drought and heatwave conditions. However, another finding is equally important and much more interesting and frequent, because it is closely associated with spells of Etesian wind outbreaks over the Aegean Sea (Prezerakos, 2022). This finding refers to cases in which the SJS is situated over the Greece mainland. Then the frontal surfaces associated with the PJS or a polar jet streak passing through Greece coming from the north cause severe weather in northern Greece, as far south as Larisa (39.39°N, 22.26°E). Precipitation does not usually occur south of Larisa because the SJS constitutes a barrier for the southward extension of the upper half of the frontal surface. In this case, cold advection occurs in the lower troposphere, resulting in a drop of temperatures even in southern Greece, due to the establishment of an Etesian wind outbreak. Thereafter, these north-easterly winds stay for a long time and weaken gradually, due to the combination of a mobile dynamic anticyclone positioned over the Balkans, after the passage of the cold front and the summer permanent Cyprus surface low. The main finding of this article is that the case of 7–10 July 2022 differs from the conceptual model mentioned above. The data used in this article are ECMWF’s operational analysis and charts from the websites of the meteorological services of Greece, Italy and Germany.

Ordinary interaction between polar and subtropical jet streams – a case from July 1998

Figure 1 is a schematic depiction which shows successive stages of the interaction between both jet streams, PJS and SJS. At stage 1 the SJS adopts a position over the Greece mainland around 38°N at 200 hPa as the northern-most limit of the Hadley cell. The PJS is shown around 45°N accompanied by a PV maximum on its poleward side. At stage 2 the SJS

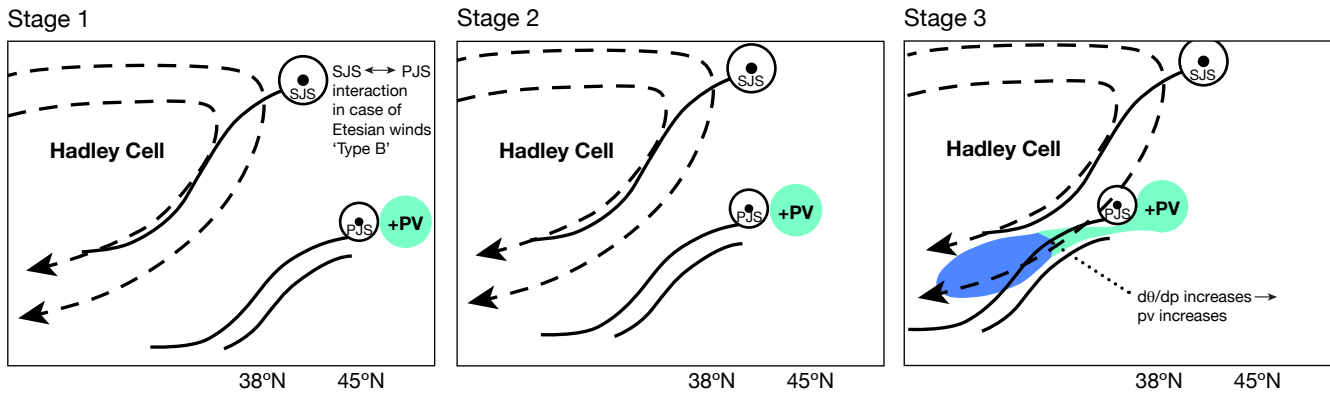


FIGURE 1 A schematic vertical cross section along 25°E from north Africa (25°N) to Europe (50°N) showing the interaction between a polar jet stream (PJS) and a subtropical jet stream (SJS) in the case of an Etesian wind outbreak. Dashed lines represent the stream lines of a Hadley cell, continuous lines represent frontal surfaces. The positions of polar and subtropical jet stream axes and maxima of PV are also shown. The charts represent three successive times starting on the left.

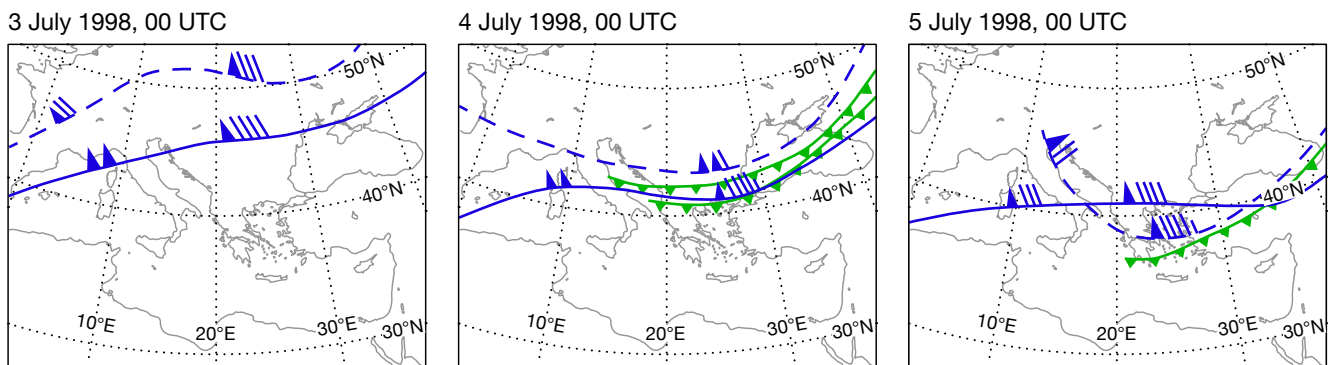


FIGURE 2 Subjective depiction of the 24 h span of the positions taken by the PJS at 300 hPa, the SJS at 200 hPa, and the surface cold front on 3, 4 and 5 July 1998 at 00 UTC. The southern second front crossing northern Greece on 4 July is shown in its position at 12 UTC. Continuous lines represent the SJS and dashed lines the PJS axis. The wind and the cold fronts are represented with World Meteorological Organization conventional symbols

remains steady, whereas the PJS has moved southwards closer to the SJS. At stage 3 a part of the PJS is just underneath the SJS, pushing it southwards. As the polar jet is stronger than the subtropical one, only the lower half of the cold frontal surface extends southwards, usually without causing precipitation over Greece to the south of the SJS, but only a drop in temperatures, with the simultaneous establishment of an Etesian winds outbreak. Figure 2 depicts the same interaction but refers to a real case, between 3 and 5 July 1998. During the last days of June and the first days of July 1998, the 2-metre temperature in Greece exhibited a continuous increase, with a peak on 3 July. The unprecedented heatwave was in the headlines. The Hellenic National Meteorological Service (HNMS) had forecast these high temperatures successfully thanks to ECMWF numerical weather prediction products. Figure 2 shows the positions of the PJS and SJS on 3, 4 and 5 July 1998. On 3 July, when 2-metre temperatures exceeded 40°C at many meteorological stations in Greece, the PJS appears to be north of 50°N, and the SJS reaches a far poleward position over the Balkans. This position is represented in

stage 1 (leftmost chart of Figure 2). See the thermodynamic equation box for an explanation of why 2 m minimum temperatures were at high levels during the first three days of July, while daytime temperatures exceeded 40°C in many Greek cities.

Significant synoptic-scale subsidence beneath and equatorward of the SJS was keeping the high mean sea-level pressure and temperatures. During the first three days of July 1998, tropical air masses cover Greece. The tropopause height is at 100 hPa and the temperature at this level is -71°C, which is also seen from records at the Hellinikon upper air station. The middle chart in Figure 2 is a good representation of the interaction process from stage 1 to stage 3 on 4 July at 12 UTC. Some precipitation and a few thunderstorms occurred in north-eastern Greece, which was to the north of the SJS axis on 4 July. After 12 UTC on 5 July 1998, an Etesian wind system was established over the Aegean Sea. Figure 3 is a visualisation of ECMWF's reanalysis fully capturing the interaction at stage 3 on 5 July 1998 at 00 UTC.

a Quantitative interpretation of the thermodynamic equation

The thermodynamic equation in a pressure coordinate system in Eulerian form is:

$$\left(\frac{\partial T}{\partial t}\right)_p = -\mathbf{V} \cdot \nabla_p T + \omega(\Gamma_\alpha - \Gamma) + \frac{1}{c_p} H \quad (1)$$

where T is the 2 m air temperature, t is time, p is barometric pressure, \mathbf{V} is the isobaric wind vector, ∇_p is the horizontal gradient on an isobaric surface, $\omega = dp/dt$ is the synoptic-scale vertical component of the wind, Γ is the actual lapse rate, Γ_α is the dry or moist adiabatic temperature lapse rate depending on whether the air is saturated or not, c_p is the specific heat of moist air at constant pressure, and H is the Newtonian heat change per unit mass and unit time caused by processes other than condensation.

All three right-hand terms of (1) contribute positively to the increase of the 2-metre temperature. On 2 July at 00 UTC, a large wave dominates the

atmospheric circulation over Europe and the Mediterranean with the main trough over the Iberian Peninsula and the main ridge over eastern Italy at 300 hPa (not shown). This synoptic situation causes (a) a warm advection toward the Balkans with maximum value over western Greece $3^\circ\text{C}/6\text{ h}$ at 850 hPa; (b) a negative advection of relative vorticity of $25 \times 10^{-10} \text{ s}^{-2}$ at the 500 hPa level over Greece, resulting in synoptic-scale subsidence of 7 hPa/h at 500 hPa and 10 hPa/h at 700 hPa; (c) in July, during the day and especially around midday, long-wave radiation from the ground increases H to extremely high values. We can conclude that, during the first three days of July, during night time the first two right-hand terms of equation (1) contribute positively to keeping 2 m minimum temperatures at high levels, due to warm advection and the synoptic-scale subsidence, while during the day the temperature exceeds 40°C in many Greek cities.

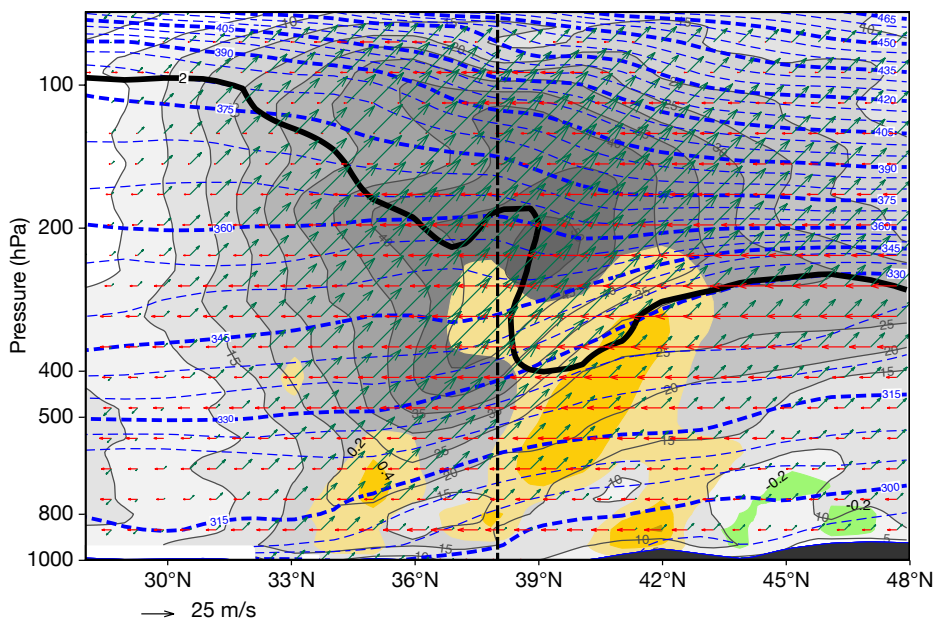


FIGURE 3 Meridional vertical cross-section along 25°E for ordinary interaction of the PJS and the SJS at stage 3 on 5 July 1998 at 00 UTC from the ERA5 reanalysis. Blue dashed lines represent potential temperature (θ) in 5 K contour intervals. Grey shading represents isotachs in 5 m/s intervals; wind speeds greater than 5 m/s are shaded. Red arrows depict the wind in the north-south direction, green arrows in the west-east direction. Colour shading represents vertical velocity in 0.2 Pa/s intervals; green shading stands for upward motion, orange shading for downward motion. The bold black line depicts the dynamical tropopause, which is defined as the height where potential vorticity reaches 2 PVU. The vertical dashed black line indicates the location of Athens.

The weather over Greece from 7 to 10 July 2022

Between 7 and 10 July 2022, the weather over Greece was particularly severe, with heavy precipitation and thunderstorms. As this period falls in the Etesian wind season, characterised by north-easterlies and synoptic-scale atmospheric stability, the phenomenon is rare but not unprecedented. The Etesian wind regime sometimes breaks down as a result of the arrival of a low-pressure system over the central and southern Aegean Sea, which is advected or more often created by temporary

cyclogenesis establishing southerly winds in its southern and eastern sectors (Prezerakos, 2022). We will try below to identify and describe the physical processes which led to this kind of weather.

On 6 July, a low-index atmospheric circulation prevailed in the north Atlantic and Europe, with a significant wave train perturbation north of 55°N showing signs of downstream development. The Azores High extended northward to just west of the British Isles, and another particularly warm subtropical anticyclone settled almost over the whole

of Europe. In summer, the permanent Persian trough extends as far as the central Aegean Sea. On 7 July, an anticyclonic breaking of the wave started just east of Britain and northwest Europe. This was used as a precursor of surface cyclogenesis over south-eastern Europe in the past. Nowadays, however, ECMWF's Integrated Forecasting System (IFS) has replaced completely all conceptual forecasting tools of this kind. The IFS accurately predicted the exact positions and the values of geopotential heights and temperatures of the wave perturbation in 500 hPa charts, as well as the 6 h cumulative precipitation amounts in almost all of Greece during the whole three-day period, even seven days in advance. This statement is based on subjective verification and the satisfaction of the general public with accurate weather forecasts, and mainly on the special alert warning issued by HNMS. At the end of the day, a 500 hPa trough accompanied by a maximum of relative vorticity appears to be just northwest of Greece moving southwards and influencing Italy and

Greece. During the morning of 8 July, severe weather occurred over most of Italy and north-eastern Greece (Figure 4). Heavy precipitation accompanied by strong lightning activity indicated the occurrence of deep convection over both countries. Surface charts obtained from the Italian Meteorological Service (not shown) depict a rather smooth low pressure field of about 1,004 hPa. They clearly mark secondary troughs and main trough centres of the wave baroclinic perturbation at 500 hPa, without any surface fronts. This fact is leading to the inference that cold advection in the upper troposphere, above a uniform warm air mass, destabilises the stratification of the atmosphere, with Convective Available Potential Energy (CAPE) building up. The release of CAPE needs trigger mechanisms to lift surface air parcels to the Level of Free Convection (LFC). These trigger mechanisms, since there is no frontal lifting, are the Greek summer sunshine heating the ground, mainly in the mountains during daytime, and the advection of relative vorticity.

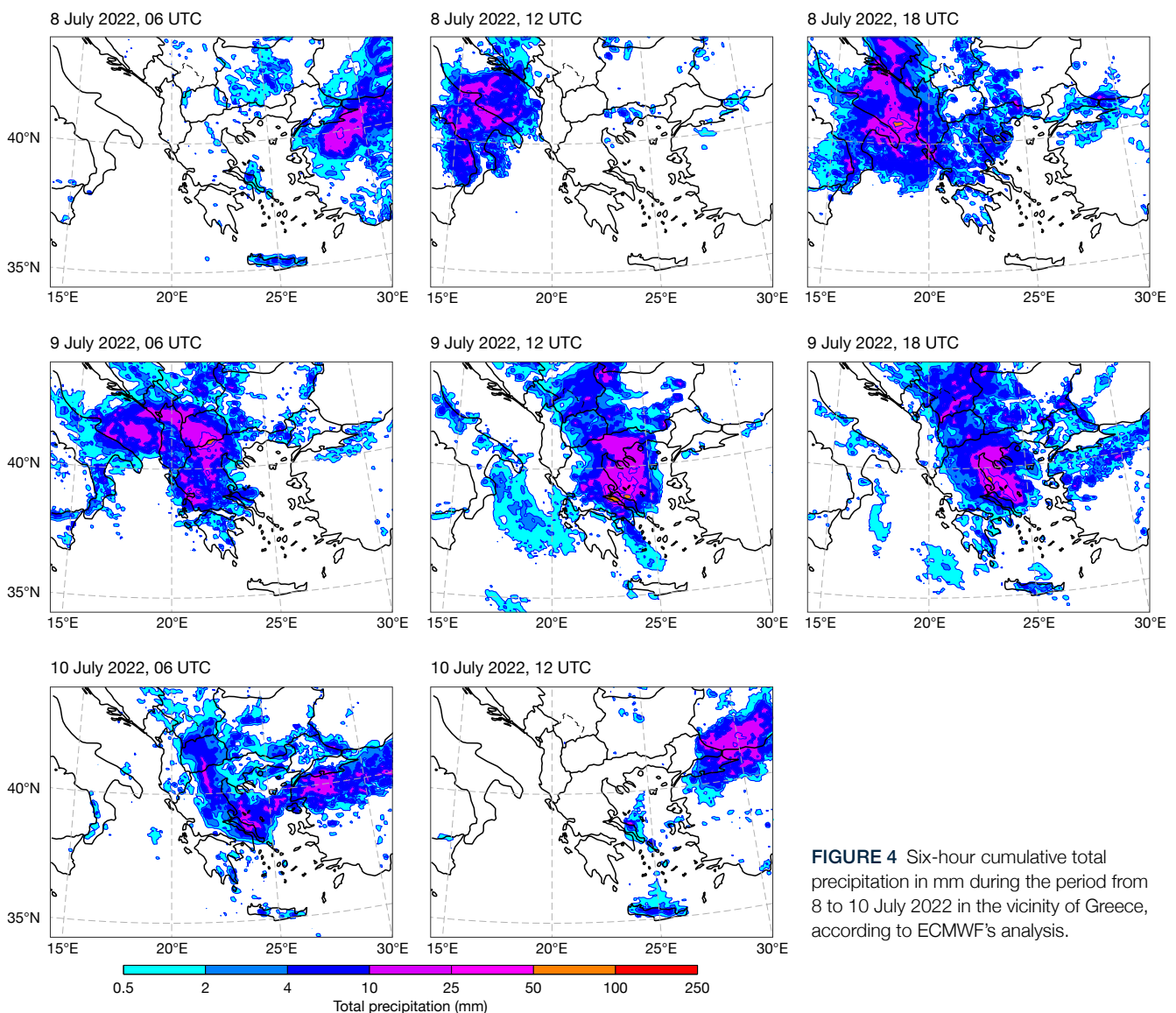


FIGURE 4 Six-hour cumulative total precipitation in mm during the period from 8 to 10 July 2022 in the vicinity of Greece, according to ECMWF's analysis.

Figure 5 presents the north–south variation of wind and temperature (θ) from 28°N to 48°N, showing the weather conditions mentioned above. On 6 July, shown in Figure 5a, the location of the SJS appears to be above 33°N at 200 hPa, extending northwards up to about 45°N. The lowering of the dynamical tropopause and the parallel flow from the north indicate the presence of a part of PJS beneath the SJS just south of 45°N. That is, the main trough of the PJS is located between the orange and green areas of opposite vertical motions. On 7 July at 12 UTC, the interaction of the two jets keeps up, resulting in the restriction of the SJS between 35°N and 40°N (Figure 5b), whereas the PJS looks to be just north of Athens, beneath the SJS. During the following two days (Figures 5c, d), the SJS core is concentrated over Crete (35°N), while the PJS advances southward on 9 July. The presence of PV greater than 2 PVU at the lower troposphere could have contributed as a trigger to releasing the existing CAPE. Finally, since the maximum of vorticity had passed the previous day, the rain over Crete on 10 July

(Figure 4) could be attributed to the release of CAPE due to heating of Cretan mountains in summer.

Concluding remarks

The analysis of weather conditions from 7 to 9 July 2022 revealed the predominance of mesoscale vertical motion compared to synoptic-scale motion. Although the ordinary interaction between the SJS and the PJS functioned pretty well, and the synoptic-scale subsidence usually occurring equatorward of the SJS axis suppressed the synoptic-scale upward motion due to the PJS, severe weather occurred over most of Greece. The combination of the warm air in the lower troposphere with the cold advection in the upper troposphere created favourable conditions for CAPE generation. The release of CAPE triggered deep convection with mesoscale upward motion. This motion is much stronger than the synoptic-scale one. The ordinary interaction is characterised by the presence of a cold frontal surface being followed by a

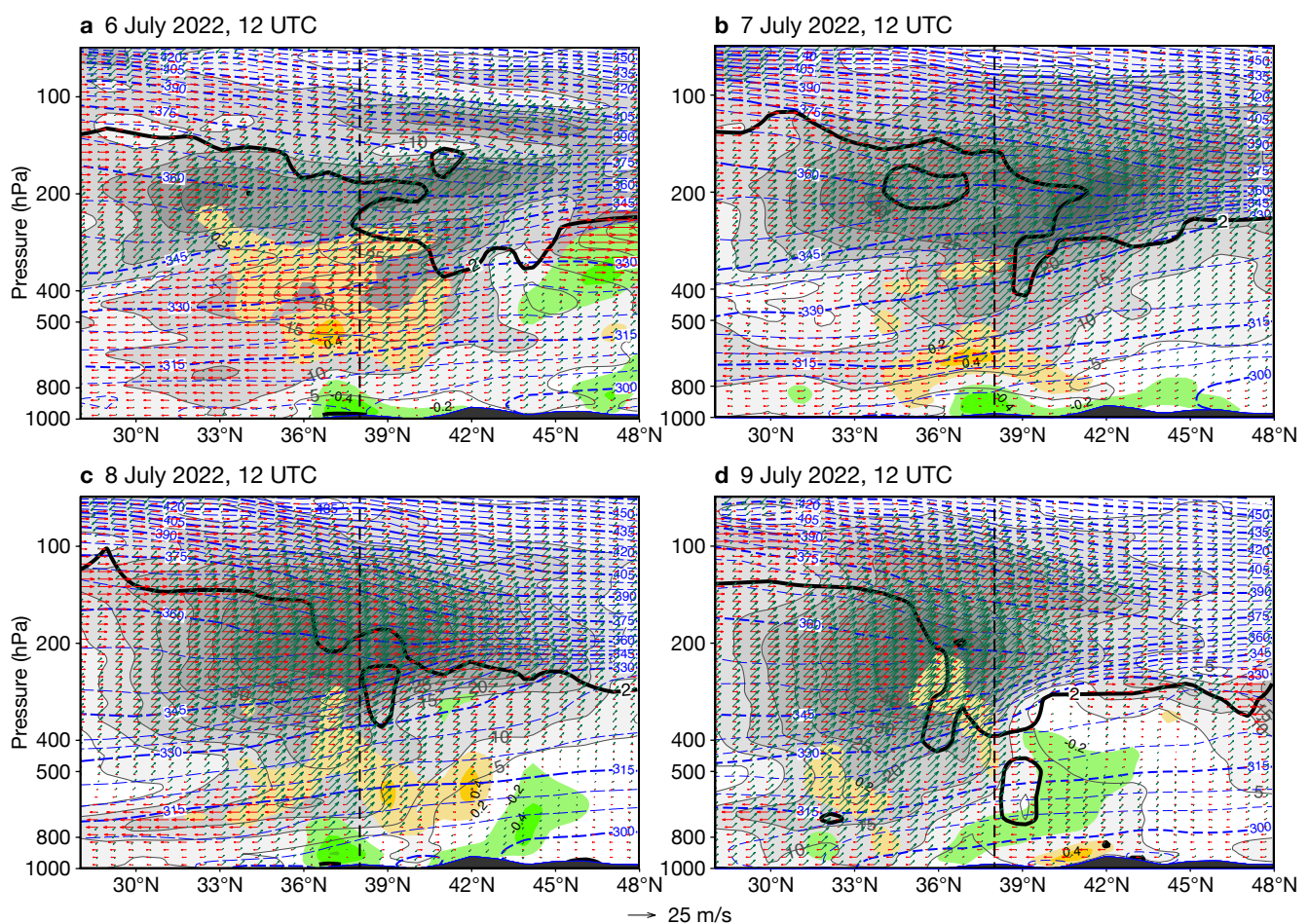


FIGURE 5 Meridional vertical cross-sections along 23°E from 28°N to 48°N on (a) 6 July 2022 at 12 UTC, (b) 7 July 12 UTC, (c) 8 July 12 UTC, and (d) 9 July 12 UTC, from the ERA5 reanalysis. As in Figure 3, the blue dashed lines represent potential temperature (θ) in 5 K contour intervals. Grey shading represents isotachs in 5 m/s intervals; wind speeds greater than 5 m/s are shaded. Red arrows depict the wind in the north–south direction, green arrows in the west–east direction. Colour shading represents vertical velocity in 0.2 Pa/s intervals; green shading stands for upward motion, orange shading for downward motion. The bold black line depicts the dynamical tropopause, which is defined as the height where potential vorticity reaches 2 PVU. The vertical dashed black line indicates the location of Athens.

b

The author and ECMWF

The 1970s were a time when the art of weather forecasting changed gradually from a semi-empirical one to a pure physical-mathematical science. The first ECMWF seminars from 1–15 September 1975, hosted by the UK Met Office College, focused on the scientific foundations of medium-range numerical weather forecasts. They were presented by invited experts from all over the world as well as ECMWF personnel. Most of the audience, including myself, realised that much of the scientific material addressed was unknown. This event provided a strong motivation for all the senior weather forecasters present to study hard to adopt all of this knowledge to become new-fashion meteorologists.

I appreciated the valuable work done at ECMWF and its continuous improvement during my time as a forecaster and then the Director of the Hellenic National Meteorological Service (HNMS) National Forecasting Centre. Just after ECMWF started disseminating its numerical products, the weather forecasts prepared by HNMS for the general public showed an amazing improvement in quality. Soon the T+48 h 500 hPa chart showed about zero root-mean-square error for Greece and neighbouring regions. This was subsequently extended to seven days or more. Hence, Greek forecasters did not need any other numerical product coming from any other meteorological centre. Later on, a limited-area model

was prepared, mainly for training purposes, by the National University of Athens and HNMS. However, its operational use was limited and temporary, and it was succeeded by COSMOGR7 and later by COSMOGR3.

In 1993, I moved to PUAS, now the University of West Attica (UNIWA), where I worked as a professor of applied mathematics and fluid dynamics. I stopped having any authority in HNMS, but I have been watching their work and kept my meteorological research interest alive. It was then that I was also appointed to be a member of ECMWF's Scientific Advisory Committee for the next eight years. Today, I know that HNMS forecasters place high trust in ECMWF's numerical products, which are used together with COSMOGR1. I would also like them to be used together with ICONGR because my experience indicates that ECMWF provides the best initial and boundary values to support limited-area models, especially in Europe.

To conclude, I would like to express my sincere thanks to ECMWF personnel for their continuous support provided to my research work, which often went beyond data access, and my best wishes for the success of ECMWF's plans for the future, which will lead to even more accurate weather forecasts for longer times ahead. I am sure this will be achieved on the basis of the excellent work having been done at ECMWF to date.

cold anticyclone moving southwards as a pair. This pair is missing in this case. The cold front does not appear at all, and the anticyclone is warm, weak and too far north from its ordinary position to be very effective. Thus the case around 9 July 2022, although it

shows an interaction of the two jets, lacks most of the other basic characteristics to be considered as ordinary. This was an exception.

The author would like to thank ECMWF scientist Ivan Tsonevsky for the revision of this article.

Further reading

Prezerakos, N.G., 1985: Synoptic scale atmospheric wave break down at 500 hPa over Europe during cold seasons, *Arch. Met. Geoph. Biocl.*, **Ser. A34**, 145–158. <https://doi.org/10.1007/BF02277444>

Prezerakos, N.G., 1990: Synoptic flow patterns leading to the generation of the north-west African depressions. *International Journal of Climatology*, **10**, 33–47. <https://doi.org/10.1002/JOC.3370100105>

Prezerakos, N.G., 2022: Etesian winds outbursts over the Greek Seas and their linkage with larger-scale atmospheric circulation features: Two real time data case studies. *Atmósfera*, **53**, 89–110. <https://doi.org/10.20937/ATM.52838>

Prezerakos, N.G. & K. Baltasis, 1977: Contribution to the study of 500 mb troughs and their relation to frontal surfaces, *Study No. 6*, Department of Research, National Meteorological Service, Athens (in Greek).

Prezerakos, N.G., S.C. Michaelides & A.S. Vlassi, 1990: Atmospheric synoptic conditions associated with the initiation of north-west African depressions. *International Journal of Climatology*, **10**, 711–729. <https://doi.org/10.1002/JOC.3370100706>

Prezerakos, N.G., H.A. Flocas & D. Brikas, 2006: The role of the interaction between polar and subtropical jet in a case of depression rejuvenation over the Eastern Mediterranean. *J. Meteorol. Atmos. Physics*, **92**, 139–151. <https://doi.org/10.1007/s00703-005-0142-Y>

WIS 2.0: WMO data sharing in the 21st century

Enrico Fucile (WMO), Jeremy Tandy (UK Met Office), Tom Kralidis (Environment and Climate Change Canada), Rémy Giraud (Météo-France)

The Global Telecommunication System (GTS) is currently the backbone of the real-time transmission of World Meteorological Organization (WMO) data globally. The Sixth World Meteorological Congress in 1971 approved the Manual on GTS and started its operational life. Since then, the GTS has proved to be a reliable real-time exchange mechanism of essential data. It provides observations to all WMO Members and Global Data-processing and Forecasting System centres, including ECMWF, as well as disseminating processed information to national meteorological and hydrological services (NMHSs). Despite some evolution of the technologies used for data exchange, the GTS has kept its basic technical foundations unchanged. The emergence of increasingly rapid, high-bandwidth global connectivity through the Internet offers new opportunities for the future evolution of the GTS. This will be achieved by upgrading the WMO Information System (WIS), which uses the GTS, to WIS 2.0. Centres migrating to WIS 2.0 will have the possibility to switch off their GTS reception and transmission equipment after the migration. The process is expected to finish by 2033, while most centres will have completed the migration by 2030.

Exchanging data through the GTS

The mechanism to exchange data through the GTS is based on a 'store and forward' mechanism. A message received by a centre is stored and forwarded to the 'next' centre in a complex point-to-point topology designed in 1969 and still operational today with very few changes. This mechanism, which predates the Internet, uses private networks to ensure the high availability of connections between NMHSs. Today, however, migrating to the Internet could provide a similar level of resilience at lower costs.

In GTS, the messages are routed from one point to another of the network using identifiers called 'GTS headers'. Based on groups of six letters, these headers are statically assigned to bulletins, and 'routing tables' are maintained in each transmission centre to direct the

messages along the planned route through the network. However, the static nature of routing tables and the relatively simple syntax of the GTS identifiers are not scalable to the current explosion in both volume and variety of data.

A further limitation of the GTS is the complexity of the topology, which requires a level of coordination between WMO Members that is sometimes difficult to reach for various technical and political reasons. However, the Internet and web technologies as a backbone for global data and information exchange offer a straightforward way to help the WMO resolve many of the fundamental data exchange issues related to the architecture of the GTS.

The WMO Information System

A significant improvement of the system was initiated by the WMO Congress in 2007 and led to the development of the WMO Information System (WIS), which was intended to complement the GTS. WIS provides a searchable catalogue and global cache to enable additional discovery, access and retrieval services through web portals maintained by 15 designated Global Information System Centres (GISCs), each operated by a WMO Member.

The WIS also defined new roles for WMO Centres worldwide, recognising the need to improve Members' coordination and facilitate data exchange beyond the World Weather Watch. However, the WIS still uses the GTS as its underlying operational service for data exchange with only minor improvements, thereby inheriting most of its intrinsic limitations.

WIS 2.0 has been designed to address the current WIS and GTS issues, to support the WMO Unified Data Policy, and to meet the demand for high data volume, variety, velocity and veracity.

WIS 2.0 principles

A set of principles is at the foundation of the WIS 2.0 technical framework and was used to define its architecture. The principles can be summarised with the following three foundational pillars:

- Simpler data exchange

- Open standards
- Cloud-ready solutions.

Simpler data exchange

WIS 2.0 prioritises the use of public telecommunication networks, unlike the private networks used for GTS links. As a result, using the Internet will enable the best choice for a local connection, using commonly available and well-understood technology.

WIS 2.0 aims to improve the discovery, access and utilisation of weather, climate and water data by adopting web technologies proven to provide a truly collaborative platform for a more participatory approach. Data exchange using the web also facilitates easy access mechanisms. Browsers and search engines allow web users to discover data without specialised software. The web also enables additional data access platforms, e.g. desktop geographic information systems (GIS), mobile applications, forecaster workstations, etc.

The web provides access control and security mechanisms that can be utilised to freely share the core data as agreed by the WMO Unified Data Policy and protect the data with more restrictive licensing constraints. Web technologies also allow for authentication and authorisation. This enables the provider to retain control of who can access published resources, and to request users to accept a licence specifying the terms and conditions for using the data as a condition for providing access to them.

WIS 2.0 uses a 'publish-subscribe' pattern, where users subscribe to a topic to receive new data in real time. The mechanism is similar to WhatsApp and other messaging applications. It is a reliable and straightforward way to allow users to choose their data of interest and to receive them reliably.

Leveraging open standards

WIS 2.0 leverages open standards to avoid building bespoke solutions that create niche markets and force NMHSs to procure special equipment. In today's standards development ecosystem, standards bodies work closely together to minimise overlap and build on their respective areas of expertise. For example, the World Wide Web Consortium provides the framework of web standards, which the Open Geospatial Consortium and other standards bodies leverage. WIS 2.0 relies on open standards with industry adoption and wide, stable, and robust implementations, thus extending the reach of WMO data sharing and lowering the barrier to access by Members.

Cloud-ready solutions

The cloud provides a reliable environment for data sharing and processing. It reduces the need for

expensive local IT infrastructure, which constitutes a barrier to developing effective and reliable data processing workflows for some WMO Members. Cloud-ready solutions that can be used in the cloud or on premises have also been developed.

WIS 2.0 encourages WMO centres to adopt cloud technologies where appropriate to meet their users' needs. Whilst WMO technical regulations will not mandate the use of cloud services, WIS 2.0 will promote the adoption of cloud technologies that provide the most effective solution.

Cloud-ready infrastructure enables easy portability of technical solutions, ensuring that a system implemented by a specific country can be packaged and deployed easily in other countries with similar needs. In addition, using cloud technologies allows WIS 2.0 to deploy infrastructure and systems efficiently, with minimum effort for NMHSs, by shipping ready-made services and implementing consistent data processing and exchange techniques.

It should be clear that hosting data and services on the cloud does not affect data ownership. Even in a cloud environment, organisations retain ownership of their data, software, configuration, and change management as if they were hosting in their infrastructure. As a result, data authority and provenance stay with the organisation, and the cloud is simply a technical means to publish and make available the data.

WIS 2.0 development and implementation methodology

WIS 2.0 adopts an improved development and implementation approach compared to WIS. The lessons learned in the first implementation of WIS and its limited success in meeting the needs of the WMO community are taken into account. A collaborative implementation approach is adopted, enabling lower barriers and increased system participation by WMO Members and partner organisations.

The development and implementation of WIS 2.0 follow five phases: setting principles; demonstration projects; architecture and drafting of technical regulations; pilot phase; and operational implementation.

Setting principles

During the initial phase, the WMO Expert Team on WIS Evolution worked on setting the WIS 2.0 Principles underpinning the technical framework. The principles were established with the WIS 2.0 strategy of creating a collaborative system of systems using web architecture and open standards to provide simple, timely and seamless sharing of trusted weather, water and climate data and information through web services.

The WIS 2.0 principles comprise a set of technical and working practices intended to modernise access to promote the discoverability and accessibility of data and information while improving the efficiency of data exchange (see Box A).

Demonstration projects

To ensure the completeness and soundness of WIS 2.0 principles and to provide material for the design of the architecture, several demonstration projects were established. They cover the areas of data exchange, data discovery, Least Developed Countries (LDC) and Small Island Developing States (SIDS), all Earth System domains and Services. The demonstration projects were established to validate and evolve the principles and provide a basis for the technical architecture. In addition, they highlighted the benefits for WMO Members and proved their effectiveness in fostering international cooperation for data sharing.

A workshop was held at the end of the demonstration projects phase, in 2021. The workshop concluded that the principles are sound and underpin data sharing at the national level and in several WMO communities. In addition, the need to develop a unifying architecture to allow interoperability between different systems was recognised and the necessity of having a reference implementation to test and validate the architecture was stated.

Architecture and drafting of technical regulations

The WMO Expert Team on WIS2 Architecture and Transition started an intense activity to finalise the technical architecture and draft the technical regulations for the Manual on the WMO Information System, which was approved in October 2022 by the Commission on Observations, Infrastructure and Information Systems (INFCOM) and finally by the WMO Congress in May 2023. In parallel, a project called 'WIS2 in a box' was initiated to provide a reference implementation to verify WIS 2.0 architecture and provide a low-cost solution for LDCs, SIDS and developing countries. 'WIS2 in a box' is Free and Open Source Software (FOSS) made available at <https://docs.wis2box.wis.wmo.int>. It is based on a cloud-ready solution, using open standards as required by WIS 2.0, and is made with Free and Open Source Software supported by active communities.

Pilot phase and operational implementation

The new WIS 2.0 data sharing framework can support the growing requirements in all WMO disciplines and domains associated with the WMO Unified Data Policy and the Global Basic Observing Network (GBON). The WIS 2.0 implementation plan was defined around the need to support these two WMO initiatives. The outcomes of the demonstration projects phase and the technical regulation drafting in conjunction with establishing the

a

The principles underpinning WIS 2.0 design

1. WIS 2.0 adopts Web technology and leverages industry best practices and open standards.
2. WIS 2.0 uses Uniform Resource Locators (URL) to identify resources (i.e., Web pages, data, metadata, APIs) use.
3. WIS 2.0 prioritises the use of public telecommunications networks (i.e., Internet) when publishing digital resources.
4. WIS 2.0 requires provision of Web service(s) to access or interact with digital resources (e.g., data, information, products) published using WIS.
5. WIS 2.0 encourages NCs (National Centres) and DCPCs (Data Collection and Production Centres) to provide 'data reduction' services via WIS that process 'big data' to create results or products that are small enough to be conveniently downloaded and used by those with minimal technical infrastructure.
6. WIS 2.0 adds open standard messaging protocols that use the publish-subscribe message pattern to the list of data exchange mechanisms approved for use within WIS and GTS.
7. WIS 2.0 requires all services that provide real-time distribution of messages (containing data or notifications about data availability) to cache/store the messages for a minimum of 24-hours and allow users to request cached messages for download.
8. WIS 2.0 adopts direct data exchange between provider and consumer and phases out the use of routing tables and bulletin headers.
9. WIS 2.0 provides a catalogue containing metadata that describes both data and the service(s) provided to access that data.
10. WIS 2.0 encourages data providers to publish metadata describing their data and Web services in a way that can be indexed by commercial search engines.

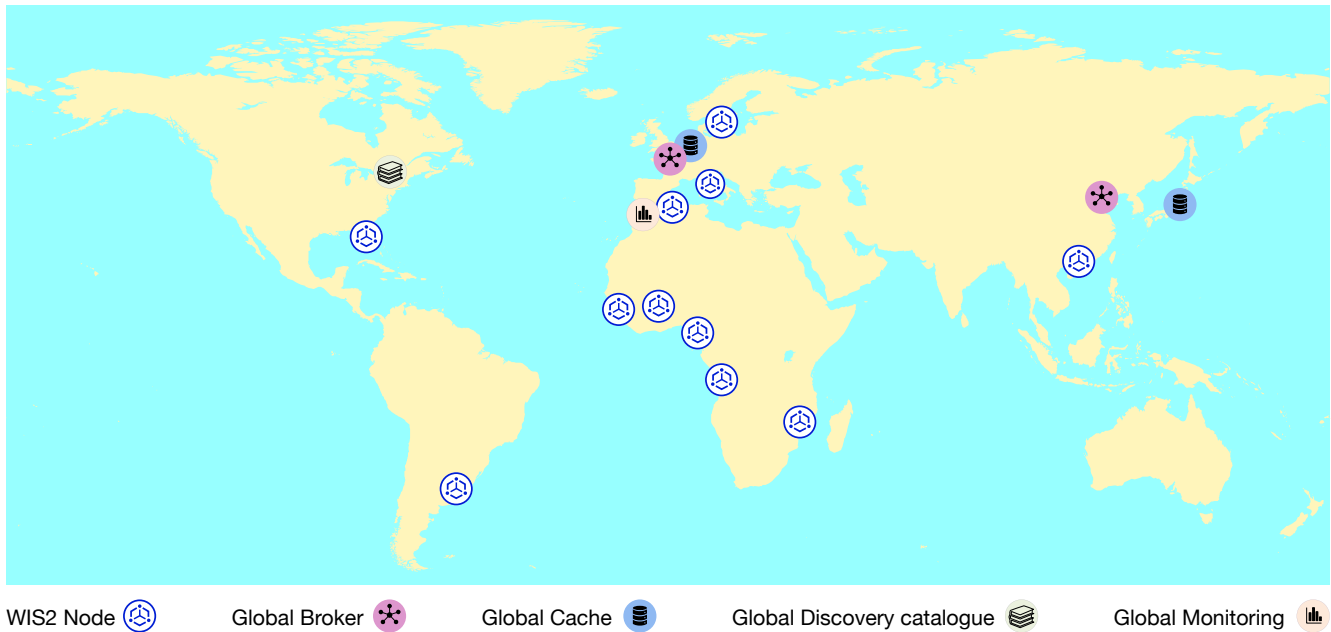


FIGURE 1 In the WIS 2.0 Pilot phase, a number of Centres are operating one service. This map shows the situation in May 2023.

‘WIS2-in-a-box’ project allowed the WMO Standing Committee for Information Management and Technology (SC-IMT) to accelerate the implementation.

A transition strategy from the GTS to WIS 2.0 was developed by SC-IMT to ensure that Centres migrating to WIS 2.0 can switch off their GTS reception and transmission equipment shortly after migrating without having to wait for the end of the migration.

The implementation has started with a one-year pilot phase in 2023, followed by a pre-operational phase in 2024, which will lead to the operational phase beginning in 2025, when WMO Members will be required to migrate from GTS to WIS 2.0. The aim is to have 90% of Members migrate to WIS 2.0 by 2030 and to switch off all the GTS infrastructure by 2033.

The various components of WIS 2.0 architecture

Every WIS Centre that is part of WIS 2.0 will operate a ‘WIS2 Node’ to receive and to send data. ‘WIS2 in a box’, introduced above, provides a reference implementation of a WIS2 Node. It should be noted that using ‘WIS2 in a box’ is not mandatory and each WIS Centre will choose the solution they see fit. Some of the WIS2 Nodes that are part of the pilot phase are using this software, others are using a solution provided by commercial partners, and some are using solutions developed in-house.

In order to provide a reliable, efficient service for all WIS users, the following Global Services have been defined:

- **Global Broker:** Centres will be responsible to make sure that all messages announcing the availability of new data and metadata can be easily obtained by all

users. The Global Broker will provide a subscription service using the MQTT (Message Queuing Telemetry Transport) standard and a Free and Open Source Software solution with additional companion software (specific to WIS 2.0) to ensure uniqueness of messages as well as verifying the correct format of those messages.

- **Global Cache:** In order to provide quick and reliable access to core data as defined by the WMO Unified Data Policy, a copy of this data will be made available by a Global Cache. Storing data from originating WIS2 Nodes, the Global Cache will then make available the core data to all WIS Users.
- **Global Discovery Catalogue:** Each dataset available on WIS 2.0 must be described by a metadata record, using the OGC API - Records standard (soon to be ratified). The Global Discovery Catalogue will provide a discovery and metadata service using Free and Open Source Software, and it will provide quality assessment capabilities in support of continuous improvement of WIS 2.0 metadata.
- **Global Monitoring:** WIS 2.0 being an operational solution, it must be monitored. Each WIS2 Node and Global Service will provide metrics relevant to their operations. Global Monitoring Centres will collect the metrics and make available a visual dashboard presenting those metrics and alert the Centres when an unexpected event occurs in support of corrective action.

At the time of writing (May 2023), the following NMHSs are operating the Global Services as part of the Pilot phase (see Figure 1):

- Chinese Meteorological Agency and Météo-France (Global Brokers)
- Japan Meteorological Agency and Deutscher Wetterdienst (Global Cache)
- Environment and Climate Change Canada (Global Discovery Catalogue)
- Maroc-Météo (Global Monitoring)

Currently the Global Broker operated by Météo-France and a WIS2 Node are being implemented in the European Weather Cloud, a federated cloud computing infrastructure set up by ECMWF and EUMETSAT.

It is planned that additional Global Services (either operated by NMHSs or the private sector) will be made

available by the end of 2023 in order to ensure sufficient redundancy of the architecture at the onset of the next phase of the implementation project, the pre-operational phase, starting in 2024.

Conclusion

After more than 50 years of operations of the GTS, and considering the data exchange challenges ahead, it is time to decommission this service and open the WIS 2.0 era. Thanks to the technical choices made based on Open Standards, the availability of a reference implementation ('WIS2 in a box'), and the commitment of experts from many NMHSs, the plan is for most NMHSs to complete the migration from GTS to WIS 2.0 in five years (2025–2030). During that period, all WMO Members and affiliated organisations, such as ECMWF, should aim to implement this new Information System.

ECMWF publications

(see www.ecmwf.int/en/research/publications)

Technical Memoranda

906 **Hotta, D., K. Lonitz & S. Healy:** Forward operator for polarimetric radio occultation measurements.
June 2023

ESA Contract Reports

Janiskova, M. & M. Fielding: Assimilation system adaptation and maintenance for cloud radar and lidar obs. *June 2023*

ECMWF Calendar 2023/24

2023

Sep 4–8	Annual Seminar
Sep 26	European Weather Cloud user workshop
Sep 27–28	Machine learning for numerical weather prediction and climate services – a workshop for ECMWF’s Member States
Oct 4–6	Scientific Advisory Committee
Oct 9–12	Training course: Use and interpretation of ECMWF products
Oct 9–13	20th workshop on high-performance computing in meteorology
Oct 19–20	Technical Advisory Committee (virtual)
Oct 24–25	Finance Committee
Oct 25	Policy Advisory Committee
Oct 30–Nov 3	Online training course: Introduction to ECMWF computing services (including MARS)
Oct 31	Advisory Committee of Co-operating States (virtual)
Nov 7	MAELSTROM Dissemination Workshop

Nov 8–10

MAELSTROM Boot Camp

Nov 13–17

Training course: A hands-on introduction to Numerical Weather Prediction Models: Understanding and Experimenting

Nov 20–24

Training course: Parametrization of subgrid physical processes

Nov 27–1 Dec

Training course: Predictability and ensemble forecast systems

Dec 7–8

Council

2024

Apr 23

Policy Advisory Committee (virtual)

Apr 23–24

Finance Committee (virtual)

Jun 19–20

Council

Oct 21–22

Finance Committee

Oct 22

Policy Advisory Committee

Dec 10–11

Council

Contact information

ECMWF, Shinfield Park, Reading, RG2 9AX, UK

Telephone National 0118 949 9000

Telephone International +44 118 949 9000

ECMWF’s public website www.ecmwf.int/

E-mail: The e-mail address of an individual at the Centre is firstinitial.lastname@ecmwf.int. For double-barrelled names use a hyphen (e.g. j-n.name-name@ecmwf.int).

For any query, issue or feedback, please contact ECMWF’s Service Desk at servicedesk@ecmwf.int. Please specify whether your query is related to forecast products, computing and archiving services, the installation of a software package, access to ECMWF data, or any other issue. The more precise you are, the more quickly we will be able to deal with your query.



Newsletter | **No. 176** | Summer 2023

European Centre for Medium-Range Weather Forecasts

www.ecmwf.int